

**ACYLATION OF ANISOLE WITH LAURIC ACID OVER
ZEOLITE BETA**

A project Report

Submitted in partial fulfilment of the requirements

For the award of the degree of

MASTER OF TECHNOLOGY

In

**CHEMICAL ENGINEERING
SPECIALISATION : CATALYSIS TECHNOLOGY**

By

CHAITANYA VIJAY DHOKE

(CH09M002)

Under the guidance of

Prof. S. Pushpavanam



**DEPARTMENT OF CHEMICAL ENGINEERING
INDIAN INSTITUTE OF TECHNOLOGY, MADRAS**

CHENNAI – 600036

MAY, 2011

CERTIFICATE

This is certify that the project report entitled “**ACYLATION OF ANISOLE WITH LAURIC ACID OVER ZEOLITE BETA**” submitted by **CHAITANYA VIJAY DHOKE** to the Indian Institute of Technology, Madras for the award of the degree of Master of technology in Catalysis Technology, Chemical Engineering is a bonafide record of the work carried out by her under my supervision. The contents of the thesis, in full or parts have not been submitted to any other institute or university for the awards of any degree.

Guide

Dr. S. Pushpavanam

Department of Chemical Engineering

IIT - Madras

Co Guide

Dr .S.SIVASANKER

National Centre for Catalysis

Research

IIT Madras

Chennai – 600 036

Date:

ACKNOWLEDGEMENT

I express my sincere gratitude to my project guide **Dr.S. Pushpavanam**. Head of chemical Engg, IIT madras for his encouragement and the guidance I received from him throughout the period of the work

I would like to thank the co guide, **Dr. S. Sivasanker**, NCCR for the guidance and encouragement given at all stages of this work. I am really grateful to him for providing opportunities to learn various aspects in catalysis I feel privileged to have been associated with him

I owe my special thanks to **Prof B. Viswanathan**, Head of NCCR for introducing me to the interesting area of catalysis. I also thank sir for providing the necessary infrastructural facilities for carrying out the research.

I am extremely thankful to **Prof. P. Selvam, Dr. K.R. Krishna Murthy, NCCR** for their constant support and invaluable suggestions during the discussions.

My Thanks goes to **Mr. T.M S Sankaranarayanan, Ms. Banu, Ms. Deepa, Ms Vijayashanti**, and **Mr. K. Suthagar** Phd scholars for their help and pleasant company during the stay in IIT madras

My classmates, especially **Mr. Sanjay, Ms. Rajalakshami, Ms. Devaki** and **Mr.Sourav** for being the pillars of support on all cloudy and sunny days.

Finally, I thank my **Parents, family** and **friends** from Mumbai for their moral support and encouragement during the period.

Chaitanya Dhoke

ABSTRACT

Friedel-Crafts acylation of aromatic compounds is used in the production of many pharmaceutical, agrochemical, and fragrance compounds. Friedel-Crafts acylation proceeds in the presence of acid catalysts. The present industrial practice involves the use of stoichiometric (or more) amounts of metal halides (Lewis acids, like AlCl_3 , FeCl_3) as the catalysts and acyl chlorides as acylation agents, which results in substantial by-product formation besides operational difficulties due to the corrosive nature of the acids and halides. To eliminate corrosion and environmental problems, the replacement of the conventional mineral acids by solid acid catalysts has become a necessity. There are many types of solid acids, such as zeolites, heteropolyacids, sulfonated resins and sulfated metal oxides that possess different acidities. Among these, zeolites are widely used as solid acid catalysts in petroleum and petrochemical processes. The wide pore zeolites, Y, beta and mordenite have found to be especially suitable for applications in the synthesis of fine chemicals.

In this work, the Friedel-Crafts acylation of anisole with a long chain carboxylic acid (lauric acid) over zeolite beta (BEA) is reported. The parent zeolite obtained from a commercial source was modified by various treatments, such as dealumination, desilication and ion-exchange to increase its activity in the acylation reaction. In the present study, the $\text{SiO}_2/\text{Al}_2\text{O}_3$ ratio (SAR = 25) of the parent BEA was altered by dealumination with HNO_3 (to SAR, 58, 88 and 170), and by desilication with tetrapropyl ammonium hydroxide (TPOH). Acidity was altered by exchanging the parent NH_4 -form with Ce^{3+} , Zn^{2+} and Fe^{3+} - ions. The samples were characterized by powder X-ray diffraction (XRD), X-ray fluorescence spectroscopy (XRF), N_2 adsorption isotherm and temperature programmed desorption (TPD) of ammonia. XRD results showed that the BEA structure was maintained after the various treatments. All the catalysts were tested in the Friedel-Crafts acylation of anisole with lauric acid. The reactions were carried out at 155°C and atmospheric pressure in two necked RB flux. Gas Chromatographic analysis of the products revealed the formation of mainly the para isomer of the ketone a [1-(4-methoxyphenyl)dodecane-1-one] as the product. The o- and m- isomers were formed in much smaller amounts. The by-products of the reaction were small amounts of phenol, methanol and unidentified compounds. While mild dealumination increased the activity, severe dealumination decreased the activity. Similarly, desilication and ion-exchange treatments also

increased the activity of the zeolite. The activity was highest for Zn-exchanged BEA. Conversion (wt %, based on lauric acid) over the parent sample (SAR = 25) was 38 %, and conversion over the other samples was: i) dealuminated BEA, 52 % for SAR 58 > 11 % for SAR 88 > 5 % for SAR 170; ii) desilicated BEA 54 % for DS1, 48 % for DS2 and iii) meta exchanged samples, 72 % for Zn-BEA, 67 % for Fe-BEA and 59 % for Ce-BEA. Likely reasons for the observed changes in activity on dealumination, desilication and ion-exchange treatments are presented.

TABLE OF CONTENTS

ACKNOWLEDGEMENTS	i
ABSTRACT	ii
LIST OF TABLES	vii
LIST OF FIGURES	viii
ABBREVIATIONS	ix
CHAPTER 1: INTRODUCTION	1
1.1 GENERAL INTRODUCTION	1
1.2 Background	1
1.3 Research Objectives	3
1.4 Scope of thesis and organization	3
CHAPTER 2: LITERATURE REVIEW	5
2.1 Acylation reaction	5
2.2 Zeolites	6
2.2.1 Zeolite Structure	8
2.2.2 Zeolite Properties	9
2.2.3 Acidity of Zeolites	11
2.3 Zeolite Beta	12
2.4 Zeolite Characterization Techniques	14
2.4.1 X-ray Diffraction (XRD)	14
2.4.2 Nitrogen Adsorption	15
2.4.3 Temperature Programmed Desorption of Ammonia (TPD)	16
2.4.4 Nuclear magnetic resonance (NMR)	17
CHAPTER 3: EXPERIMENTAL METHODOLOGY	18
3.1 Chemicals	18
3.2 Instruments	18
3.3 Preparation of catalysts	18
3.3.1 Modification of zeolite beta for acylation reaction	18
3.3.1.1 Dealumination procedure	19
3.3.1.2 Desilication procedure	19
3.3.1.3 Preparation of Ion exchange beta	19
3.3.1.3.1 Ion-exchange of BEA(25) with Fe ³⁺ ions	19

3.3.1.3.2 Ion-exchange of BEA(25)with Zn ³⁺ ions	19
3.3.1.3.3 Ion-exchange of BEA(25)with Ce ³⁺ ions	20
3.3.2 Catalyst preparation for hydrogenation reaction	20
3.3.2.1. Impregnation with Pd	20
3.3.2.2 Impregnation with Ru	20
3.3 Characterization techniques	22
3.3.1 X-ray Diffraction	22
3.3.2 Solid State NMR spectroscopy	22
3.3.3 Nitrogen Adsorption	22
3.3.4 Temperature programmed desorption (TPD) of NH ₃	23
3.4 Catalytic Test	23
3.4.1 Acylation of Anisole with lauric acid over BEA catalysts	23
3.4.2 Product Identification	25
3.4.3 Hydrogenation of Anisole and acetophenone	25
CHAPTER 4: RESULT AND DISCUSSION	26
A. ACYLATION OF ANISOLE WITH LAURIC ACID	26
4.1 Physicochemical characterization of BEA samples	26
4.1.1 Compositional analysis of the samples	26
4.1.2 XRD studies of modified BEA samples	27
4.1.3 Surface areas and pore volume by N ₂ sorption	30
4.1.4 Acidity of dealuminated samples from TPD of NH ₃	33
4.1.5 ²⁷ Al MAS NMR spectrum of BEA(25)	33
4.2 Catalytic Activity of Zeolite Beta in Friedel-Crafts Acylation	34
4.2.1 Influence of changing the SAR	35
a. Effect of Dealumination	35
b. Effect of Desilication	38
4.2.2 Influence of Ion Exchange	39
4.2.3 Effect of External Mass Transfer	40
4.2.4 Effect of Temperature	43
4.2.5 Effect of molar ratio (Anisole: C ₁₂)	45
B. HYDROGENATION OF ANISOLE AND ACETOPHENONE	46
4.3 Hydrogenation studies	46
4.3.1 Characterization of the Catalysts	47
4.3.2 Hydrogenation reactions	47

4.3.3 Hydrogenation of Anisole	48
4.3.4 Hydrogenation of Acetophenone	50
4.3.5 Comparison of initial rates	53
CHAPTER 5 CONCLUSION	55
REFERENCES	58

LIST OF TABLES

TABLE NO.	TITLE	PAGE NO.
3.1	Conditions used in the dealumination of beta	19
3.2	Conditions of desilication	20
4.1	Compositional analysis by XRF spectroscopy	27
4.2	Relative crystallinities of the parent and dealuminated samples	28
4.3	Surface areas and pore volumes of the dealuminated and desilicated BEA samples.	32
4.4	Acidity of dealuminated BEA from TPD of NH ₃	33
4.5	Product distribution for acylation reaction on different modified BEA samples	36
4.6	Product distribution in hydrogenation of anisole over different catalysts	50
4.7	Product distribution in hydrogenation of acetophenone over different catalysts	51
4.8	Comparison of the initial rates for acylation and hydrogenation reaction	53

LIST OF FIGURES

FIGURE NO.	TITLE	PAGE NO.
2.1	Primary Building Unit (PBU) : $[\text{SiO}_4]^{4-}$ or $[\text{AlO}_4]^{5-}$	8
2.2	Schematic representative of the building of zeolite framework	9
2.3	Bronsted and Lewis acid sites in zeolite framework	12
2.4	Zeolite beta framework viewed along a) [100], b) [001]	13
2.5	The six types of adsorption-desorption isotherms for microporous and mesoporous materials.	15
3.1	Pictorial representation of the batch reactor used	24
3.2	Scheme for the acylation of anisole with lauric acid	24
4.1	XRD patterns of the dealuminated samples and the parent zeolite	28
4.2	XRD patterns of the desilicated samples and parent zeolite	29
4.3	XRD patterns for metal loaded BEA samples and parent BEA	30
4.4	Adsorption-desorption isotherms of parent BEA	31
4.5	^{27}Al spectra of the parent BEA used in the studies	34
4.6	Effect of dealumination on acylation reaction	36
4.7	Effect of desilication on acylation reaction	38
4.8	Effect of metal ion-exchange with cation on acylation reaction	39
4.9	Effect of RPM to study external mass transfer in film	41
4.10	Effect of temperature on acylation reaction	43
4.11	Arrhenius plot for acylation reaction	44
4.12	Effect of Molar ratio on acylation reaction	46
4.13	X-RAY diffraction pattern for metal loaded on beta BEA (58)	47
4.14	X-RAY diffraction pattern for metal loaded on NaY (58)	48
4.15	Hydrogenation of anisole	49
4.16	Scheme for formation of the observed products in the hydrogenation of anisole	49
4.17	Hydrogenation of acetophenone	51

ABBREVIATIONS

BEA(25)	Zeolite Beta with SiO ₂ /Al ₂ O ₃ ratio = 25 obtained from Zeolyst
BEA(58)	Dealuminated sample by treatment of 10 % nitric acid at Room temperature for 1h
BEA(88)	Dealuminated sample by treatment of 10 % nitric acid at Room temperature for 6h
BEA(170)	Dealuminated sample by treatment of 10 % nitric acid at 80 ⁰ C for 6h
BEA(-)	Desilicated sample by treatment with 20 ml TPAOH at 70 ⁰ C for 4h
BEA(-)	Desilicated sample by treatment with 30 ml TPAOH at 60 ⁰ C for 4h
BEA-Fe	BEA(25) ion exchanged with Fe
BEA-Zn	BEA(25) ion exchanged with Zn
BEA-Ce	BEA(25) ion exchanged with Ce
0.5%Pd/BEA(58)	0.5% Palladium (Wt. basis) loaded on BEA(58)
0.5%Ru/BEA(58)	0.5% Ruthenium (Wt. basis) loaded on BEA(58)
0.5%Pd/NaY()	0.5% Palladium (Wt. basis) loaded on NaY()
TPAOH	Tetrapropyl ammonium hydroxide
C ₁₂	Lauric acid
BET	Brunnauer, Emmet and Teller
FTIR	Fourier transform infrared spectroscopy
GC	Gas Chromatography
Pd	Palladium
Ru	Ruthenium
Fe	Iron
Zn	Zinc
Ce	Ceria
SBA	Secondary building unit
PBU	Primary building unit
TPD	Temperature programmed desorption
Wt.	Weight
wt %	Weight %
XRD	X-Ray Diffractogram
NMR	Nuclear magnetic resonance
E _a	Activation energy
T	Temp in Kelvin

R	Universal gas constant
r_a	Rate of reaction with respect to a
R_{obs}	Observed rate of reaction
X_a	Fractional conversion
[A]	Concentration of A
[B]	Concentration of A
[A ₀]	Initial concentration of A
[B ₀]	Initial concentration of B
[A _s]	Concentration of A at surface of catalysts
[B _s]	Concentration at surface of catalysts
a_p	Particle surface area per unit liquid volume
k_a	Mass transfer coefficient for A
K_b	Mass transfer coefficient for B
RPM	Revolution per minute
Sh	Sherwood number
d_p	Particle diameter
Dimeric ketone	2-cyclohexylcyclohexanone
A/LA	Anisole to lauric acid in mole
Vol_{meso}	Mesoporous volume
$Area_{meso}$	External surface area

1. INTRODUCTION

1.1 GENERAL INTRODUCTION

Chemical process industry is a large industry with a global turnover of US \$1400 billion per year (Roland *et al.*, 1996). It has been recognized that the status of the chemical process industry is a reliable indicator of the country's state of industrialization. It is well known that the chemical process industry is mainly based on catalytic processes. More than 90% of all the chemical products manufactured involve at least one catalytic step, often several catalytic procedures (Holderich *et al.*, 1997). Zeolite acid catalysts have a wide application in industrial processes such as alkylation, acylation, isomerization, amination, cracking etc. (Holderich *et al.*, 1999). According to these authors, zeolites are among the most used catalysts in industrial processes. The utility of zeolites as catalysts in organic processes has been investigated by many researchers. Beta is a typical example of a zeolite with high activity in many reactions used in fine chemical production, such as alkylation (Chiu *et al.*, 2004), acylation (Casagrande *et al.*, 2000) and other hydrocarbon transformations (Absil *et al.*, 1998). Zeolites possess acid sites at the framework (surface), which can catalyse reactions involving organic cations, such as Friedel-Crafts reactions, cracking and isomerization. The acid sites in zeolites are associated with the tetrahedral aluminium atoms in its framework (Zaiku *et al.*, 2002), and, therefore, the amount of acidity depends on the aluminium content of the zeolite. Besides, the key opportunity for the use of zeolites as catalysts relies on their unique pore dimensions, which can control the selectivity of the reaction. In view of their non-corrosive nature and many environmentally attractive features, zeolites are employed as alternative solid acid catalysts, replacing homogeneous mineral acids, particularly in Friedel-Crafts reactions.

1.2 BACKGROUND

Friedel-Crafts acylation of aromatics is an important basic reaction in the production in many pharmaceutical, agrochemical and fragrance compounds, since aromatic ketones are the intermediates in the production of many of these compounds. For example, 6-acyl-2-methoxynaphthalene, 4-acyl-anisole and 4-acyl-veratrole are the products of regio selective acylation of the respective aromatic ethers. Present

industrial practice involves the use of more than stoichiometric amounts of metal halides (e.g. AlCl_3 , FeCl_3) as the catalysts and acyl chlorides as acylating agents, which results in a substantial amount of by-products, besides corrosion problems. The large amount of catalyst usage is related to the stronger coordination of the formed aromatic ketone to the Lewis acid catalyst compared to the acid chloride. Thus the association constant of FeCl_3 was found to be 100 times larger for the ketone than for the corresponding chloride. The inherent disadvantages in the use of conventional Lewis acid metal chlorides for Friedel Crafts acylation are that they are non regenerable and require more than stoichiometric amounts due to the complex formation with the acylating agent as well as the carbonyl product. Work-up to decompose the resultant intermediate complex by hydrolysis forms a large amount of waste product. Alternatively, strong acids, e.g. hydrogen fluoride, are used in the industrial practise. Therefore, the application of heterogeneous (solid acid) catalysts becomes very attractive due to the simple separation of the products and the possibility of regenerating and reusing the catalysts. Also, elimination of corrosion and environmental problems can be achieved by replacement of the conventional catalysts, such as AlCl_3 , by solid acid catalysts. In the literature, solid acids like ion exchanged clay, sulphated zirconia, and large number of zeolite catalysts have been described as active catalysts in the acylation of aromatics. The most common zeolites for acylation are zeolite Y (FAU, mostly dealuminted), beta (BEA) and ZSM-5 (MFI). The first industrial application of solid acids in acylation, introduced by Rhodia, is the liquid phase acylation of anisole and veratrole with acetic anhydride over H-Y and H-BEA zeolites in a recycle fixed-bed reactor (Beer *et al.*, 2001).

In this work, we have chosen zeolite beta (BEA) to be studied as the catalyst in view of recent developments in the application of heterogeneous catalysts in Friedel-Crafts reaction. BEA has a great potential as an industrial interest because of its strong acidity, large pore ($\sim 7.0 \text{ \AA}$) dimensions, large silica content and high thermal stability. The acidity of a zeolite is an important topic in the study of zeolite catalysis. The acid sites in zeolites are linked to the tetrahedral aluminium atoms in the framework of the zeolite (Zaiku *et al.*, 2002). Though zeolites are, therefore, expected to possess mainly Brönsted (protonic) acidity, the commercial sample used in this study has been reported to possess both Brönsted and Lewis acid sites, the Lewis acid sites arising from extra framework Al-specie. Studies have shown that the amount of Brönsted and Lewis acid sites determine product selectivity in Friedel-

Crafts reactions (Narayanan *et al.*, 2001; Sultana *et al.*, 1998; Nivarthi *et al.*, 1998; Yadav *et al.* 2003). Therefore, in this study the acidity of BEA will be modified by varying the altering the Al-content of the zeolite by dealumination and desilication treatments and by exchanging framework NH_4^+ ions (precursors to protonic acidity) with Ce^{3+} , Zn^{2+} and Fe^{3+} ions.

1.3 RESEARCH OBJECTIVES

The objectives of this study are:

1. To modify zeolite beta for different Si/Al ratios by dealumination and desilication.
2. To modify the acidity of zeolite beta by introducing Ce, Zn and Fe ions.
3. To characterize the modified zeolite samples with respect to their Si/Al ratios, N_2 adsorption and acidity characteristics.
4. To test the reactivity of the modified zeolite samples in Friedel-Crafts acylation of anisole with lauric acid (i.e. C_{12} acid) to yield the ketone.
5. Study the hydrogenation of the aromatic ketone (or a model ketone) and anisole using supported metal bi-functional catalysts. If a suitable catalyst is identified, carry out the acylation and hydrogenation of the ketone in a single step to produce other products.

1.4 SCOPE OF THE THESIS AND ORGANIZATION OF THE CHAPTERS

The major objective of this work is to study the acylation of anisole with lauric acid over zeolite beta and its modified forms. Zeolite beta was modified by dealumination and desilication and by ion-exchanging with metal ions, viz. Ce^{3+} , Zn^{2+} and Fe^{3+} . The catalysts were then characterized and used in the Friedel-Crafts acylation of anisole with lauric acid. The reaction was performed in a batch reactor and the product was analysed by gas chromatography (GC). Also, a study of the hydrogenation of an aromatic ketone and anisole was done using Pd and Ru supported on acidic BEA and a basic zeolite (NaY).

Chapter 1 – Presents an introduction to the topic of research. The motivation behind this work has been discussed. The objectives of this research work and a broad outline of the organisation of the thesis are also presented.

Chapter 2 – A general overview of the pertinent literature with critical assessment of the status of research relating to the problem under consideration.

Chapter 3 – The methods used in the preparation of the catalysts and their characterisation techniques are discussed.

Chapter 4 – The results of the characterization of the various BEA samples used in this study are reported. Studies on the catalytic activity of BEA and modified BEA samples in the Friedel-Crafts acylation of anisole with lauric are presented. The influence of reaction parameters on the acylation reaction is presented. Studies on the hydrogenation of anisole and the model aromatic ketone, acetophenone, over zeolite supported metal catalysts are presented.

Chapter 5 - A summary of the results and broad conclusions of the present work are presented.

2. LITERATURE REVIEW

2.1 ACYLATION REACTION

Friedel-Crafts acylation of aromatic compounds is used to produce aromatic ketones that find numerous applications in the manufacture of fine chemicals, fragrances and pharmaceuticals. Current industrial acylation processes mostly use mineral acids (e.g., AlCl_3 , BF_3 , and FeCl_3) as catalysts and acyl halides as acylating agents. The major drawback in the conventional manner of making aromatic ketones is the need to use stoichiometric (or more) amounts of the Lewis acid, their separation, disposal of the acids, and the corrosive nature of the acyl halides and the acids. Therefore, it is greatly beneficial to carry out the reactions using carboxylic acids or carboxylic acid anhydrides as raw materials instead of acyl halides and non-toxic and easily separable solid acids as catalysts. Typical solid acid catalysts that can be used in acylation reactions are sulphated zirconia, Nafion-H, Nafion/silica, pillared clays, rare earth exchanged pillared clays, Keggin-type heteropolyacids, and medium and large pore zeolites (like HY, H-beta).

Botella *et al.* studied the use of zeolite beta for the synthesis of 4-methoxyacetophenone by acylation of toluene with acetic anhydride and got almost 95% of the acylation product selectively. They found that the inhibition step was desorption of the ketone, which was reduced by using an excess amount of toluene as it helped in desorbing the ketone. The reaction was studied in the temperature range of 140-250 °C. Vidhya *et al.* studied the acylation of anisole by acetic anhydride over a porous solid acid (Nafion SAC-13) and a heteropolyacid (HPA) to yield p-methoxyacetophenone (PMOAP), they got more than 95% selective product with 45-50% conversion of anhydride. Reaction conditions were 120 bar pressure, temperature 70°C, anisole : anhydride ratio 5:1, space velocity of $1.6 \text{ g}_{\text{acetic anhydride}} \text{ g}_{\text{cat}}^{-1} \text{ h}^{-1}$. But both of these catalysts got deactivated in liquid phase operation within 24 hrs, and the reason for the deactivation proposed for HPA was leaching of the Keggin ion, while for SAC-13, it was the adsorption of PMOAP in the micro pores of the Nafion catalyst. SAC-13 was treated with boiling HNO_3 solution to restore its complete activity.

Boyapati *et al*,1997,studied the acylation of aromatic ethers with acid anhydride in the presence of cation exchanged clay, K10 montmorillonite, ($\text{M}^{\text{n}+}$ -

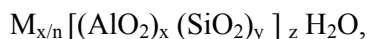
mont., where $M^{n+} = Fe^{3+}, Zn^{2+}, Cu^{2+}, Al^{3+}$ and Co^{2+}) and found Fe^{3+} & Zn^{2+} exchanged montmorillonite were more active than the others. The authors also discussed the effect of temperature and solvent in the acylation of anisole and veratrole. Hiroshi Y.*et.al.* 2010. investigated the acylation of aromatic compounds using carboxylic acids and zeolite (H-Y & H-beta) with microwave irradiation. The advantage of using carboxylic acid is that the co-product is water, thus, making it a 'green' and environment friendly reaction. The authors also found that acylation using a solid acid was effectively accelerated by using microwave irradiation rather than a conventional oil bath reaction. They studied the acylation of anisole using hexanoic acid, butyric acid and propionic acid at 190 °C and 2.45 GHz and obtained promising results for hexanoic and butyric acids, but the reactivity was low for propionic. Activation energy for the reaction of butyric acid and anisole by microwave and oil bath heating was also estimated.

Beer *et al.*, 2001 studied a number of zeolites (H-beta, H-Y and Nafion/silica) for the acylation of aromatics. The mesoporosity of the catalyst and the Si/Al ratio was shown to be very important in the acylation reaction. They studied the reaction with and without removal of water, and got good conversion (i.e. 80%) when water was removed from the process, thus, showing that water formation was the inhibition step when carboxylic acid was used as the acylating agent. An integrated reactor configuration was used to remove water by the counter current stripping by gases. As the catalyst was coated on a thin layer over the reactor wall, this configuration gave less yield than slurry reactors due to the limited amount of active sites being available for the reaction. Waghlikar *et al.* 2007 investigated the acylation of anisole with long-chain carboxylic acids over wide pore zeolites. The acylation reaction was influenced by the type of zeolite and the chain length of the carboxylic acid. They found that the activity of the zeolite was increased by dealumination which they attributed to the formation of mesopores, which decrease the diffusion resistance of the zeolite.

2.2 ZEOLITES

Zeolites are microporous crystalline aluminosilicates that have been studied by mineralogists for more than 200 years. They are comprised of channel and cavities of

molecular dimensions ranging from 3 to 10 Å in diameter. The general formula for the composition of a zeolite in the hydrated form is:



where M is an extra framework cation that balances the anionic charge of the framework, n is the valency of M, x and y are the total number of aluminate and silicate tetrahedra per unit cell and z is the number of water molecules in one unit cell. Typical cations include alkali metals, e.g. Na⁺, K⁺, alkaline earth metals, e.g. Ca²⁺, Ba²⁺ and other cations such as NH₄⁺ and H⁺ (Breck *et al.*, 1974). Stilbite is a natural zeolite that was first discovered in 1756 by a mineralogist from Sweden, Alex Fredrich Cronstedt. Cronstedt named the mineral as “zeolite” which originates from the Greek words “zeo” means boiling and “lithos” means stones because it swells and evolves steam when fused in the blowpipe (Breck, *et al.*, 1974). After that, many natural zeolites were discovered such as mordenite, clinoptilolite, natrolite, chabazite, heulandite, faujasites and others. Numerous synthetic zeolites have also been synthesized.

With the great demand of zeolites for commercial applications, zeolites are produced synthetically in large industrial quantities. More than 150 zeolites have been synthesized. Synthetic zeolites were first prepared in the 1950s by the Union Carbide Corporation USA. Several types of zeolites were synthesized commercially such as zeolite A, X, Y, mordenite and ZSM-5. Zeolite Y and zeolite X have found many catalytic applications in petroleum and petrochemical industries (Anonymous, 2001). Sodium type A, zeolite Na-A, has a mean pore diameter of 4-6 microns and is suited excellently for exchange of calcium ions. Consequently it is used as a detergent builder.

Another synthetic zeolite, ZSM-5, developed by Mobil in the mid 1960s has become an important catalyst in many petroleum and petrochemical processes. The development of ZSM-5 type catalysts has allowed octane enhancement in catalytic cracking (Barrer *et al.*, 1982). The different zeolites are distinguishable from each other on the basis of composition, crystal structure and sorption properties. The properties of zeolites that are exploited commercially are adsorption, catalytic activity and ion exchange. Catalysis is a major area of usage for synthetic zeolites. Several catalysts developed during the 1960s have revolutionized petroleum refining and petrochemical processes. Molecular sieving and shape selectivity became possible with the synthetic zeolites. Shape selective catalysis can be performed inside the zeolite's cavities to give a single product (Breck *et al.*, 1974).

2.2.1 ZESOLITE STRUCTURE

Zeolites are crystalline aluminosilicate compounds based on an infinitely extending three dimensional framework of tetrahedrally coordinated SiO_4 and AlO_4 species linked by corner shared oxygen ions (Flanigen *et.al.*, 1991). The primary building unit of zeolite structure is a tetrahedron composed of a central Si or Al atom surrounded by four oxygen atoms, namely $[\text{SiO}_4]^{4-}$ or $[\text{AlO}_4]^{5-}$ (Barrer *et.al.*, 1982). These tetrahedral units referred to as primary building units (PBU) (Fig 2.1) are assembled into secondary building units (SBUs) (Fig 2.2), which are then assembled and organized to form the structural framework of zeolites. These tetrahedra are linked through the oxygen atoms, subject to the condition (Lowenstein's Rule) that no two aluminum atoms can share the same oxygen, to form 3-dimensional framework structures containing channels and cages of discrete size.

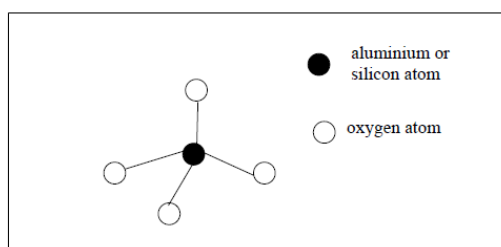


Fig 2.1 Primary Building Unit (PBU): $[\text{SiO}_4]^{4-}$ or $[\text{AlO}_4]^{5-}$

As a result of the charge difference between the $[\text{SiO}_4]^{4-}$ and $[\text{AlO}_4]^{5-}$ tetrahedra, the framework charge, when aluminium atoms are contained in the zeolite, is negative and hence must be balanced by cations, typically alkali or an alkaline earth ions. As these cations are loosely bound to the framework and are present in the voids in the structure, they can be easily exchanged by conventional ion-exchange methods. The position, size and the number of cations can significantly alter the properties of the zeolite. When the cations are protons (H^+), Brönsted acid sites are created. These zeolites are acidic and are capable of acid catalysis, such as cracking, alkylation, acylation, dehydration and isomerization reactions.

Zeolite pores (channels in the framework structure) mostly consist of 8, 10 and 12 members of oxygen ring systems and may extend in one, two or three directions. Zeolites can be classified according to the diameter of their pores (\AA); small pore zeolites, which possess 8-membered oxygen ring systems with $\text{\AA} < 4.5$, such as zeolite A, chabazite and erionite; medium pore zeolites, which possess 10 membered

oxygen ring systems with $4.5 \text{ \AA} < \emptyset < 6.5 \text{ \AA}$, such as ZSM-5, ferrierite and TS-1; and large pore zeolites with 12-membered oxygen ring systems with $\emptyset > 6.5 \text{ \AA}$, such as mordenite, faujasite, ZSM-12, and beta (BEA) (Flanigen *et al.*, 1991). Zeolites are identified by a three letter code (assigned by the International Zeolite Association; IZA) based on the uniqueness of their structure; e.g. MOR for mordenite, MFI for ZSM-5, FAU for zeolites X and Y, and BEA for zeolite beta.

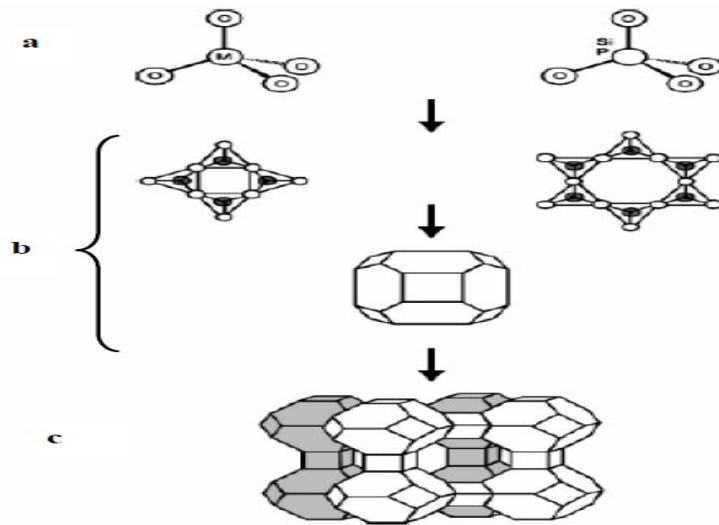


Fig 2.2 Schematic representative of the building of zeolite framework

a) Primary Building Units b) Secondary Building Units c) Structure of zeolite A

2.2.2 ZEOLITE PROPERTIES

Zeolites with alkali and alkaline earth metal cations are normally colorless crystalline powders. Color may occur in zeolites if they contain transition metals impurities or if they have been modified by ion exchange with these elements. The primary particle size is typically in the range of 0.1-15 μm . Single crystals often form larger aggregates. On heating, hydrated zeolites release water. Most zeolites can be completely dehydrated without major alterations to their framework by calcination at 400-500°C. The density of zeolites is low, ranging from about 1.9-2.3 g/cc. Cation exchange with heavy ions increases the density; some barium zeolites have densities as high as 2.8 g/cc. The density depends on the openness of the zeolite structure and the cation (Breck *et al.*, 1974). The thermal stability is seen to increase with increasing $\text{SiO}_2/\text{Al}_2\text{O}_3$ ratio of the framework. In low silica zeolites ($\text{SiO}_2/\text{Al}_2\text{O}_3 < 5$) the crystalline decomposition temperature is near 700 °C, while in high silica zeolites

the crystalline decomposition temperature can be above 1300 °C. The acid or base stability of zeolites also varies with the framework $\text{SiO}_2/\text{Al}_2\text{O}_3$ ratio. Low silica zeolites are fragile in the presence of acids, while high silica zeolites are completely stable in boiling, concentrated mineral acids. Conversely, high silica zeolites are unstable in basic solution, while low silica zeolites show increased stability (Murphy *et al.*, 1996).

The aluminium in the zeolite tends to make the zeolite hydrophilic. With increasing silica content and decreasing aluminium, the zeolite becomes more hydrophobic and therefore the greater the ability of these materials to interact with hydrophobic organic molecules or to exclude hydrophilic molecules, such as water. The transition from hydrophilic to hydrophobic occurs at about $\text{SiO}_2/\text{Al}_2\text{O}_3 = 20$. Whether zeolites are hydrophilic or hydrophobic can have a profound influence on their chemical reactivity (Juttu *et al.*, 2001). Zeolite has an ion exchange property which was first observed more than 100 years ago. Because of their three dimensional framework structure, most zeolites do not undergo any appreciable dimensional change with ion exchange. One application for commonly occurring zeolite minerals such as clinoptilolite is in the selective removal of radioactive ions from radioactive waste materials. The cation exchange behaviour of zeolites depends upon the nature of the cationic species, the cation size, both anhydrous and hydrated, cation charge, the concentration of the cations in solution and the structural characteristics of the particular zeolite (Breck *et al.*, 1974).

Zeolite also plays a role as a molecular sieve, when there are adequate shape and size differences between the molecules to be separated. Guest species of the right shape and size penetrate readily, but molecules of the wrong shape or size can be totally excluded (Barrer *et al.*, 1982).

2.2.3 ACIDITY OF ZEOLITES

Acidity is one of the most important characteristics of zeolites, which makes them very useful in acid catalysis. A good understanding of the nature and number of acid sites in a zeolite is needed in order to develop improved and novel catalysts for applications in chemical industries (Juttu *et al.*, 2001). The reactivity and selectivity of zeolites as acid catalysts are determined by the strength and number of the acid sites (Costa *et al.*, 2000). The framework aluminium atoms are negatively charged and balanced by extra-framework cations that are (or potential) active acid sites

(Barrer *et al.*, 1982). The acidic properties of zeolites are mainly dependent on the Si/Al molar ratio as well as the temperature of activation. In zeolites, acid sites are classified according to the classical Brønsted and Lewis acid models (refer to Fig 2.3). Brønsted acidity corresponds to proton donor acidity, while Lewis acidity corresponds to an electron pair acceptor. Brønsted acidity occurs when the cations used to balance the negatively charged framework are protons (H^+). A trigonally coordinated aluminium atom possessing a vacant orbital that can accept an electron pair, behaves like a Lewis acid site. To produce acidic zeolite catalysts, it is necessary to replace the cations present in the freshly synthesized material with protons. In zeolites, protons can be introduced by various methods. If an aluminium ion, which is trivalent, is substituted isomorphously for a silicon ion, which is quadrivalent, in a silica lattice comprising silica tetrahedra, the net negative charge must be stabilized by a nearby positive ion such as a proton. This positive ion can be produced by the dissociation of water, forming a hydroxyl group on the aluminium atom. The resulting structure, in which the aluminium and the silicon are both tetrahedrally coordinated, side by side produces Brønsted acid. If this structure is heated occluded water in the zeolitic framework is driven off followed by condensation process and Brønsted acid sites are converted to Lewis acid sites. Some metal atoms are now three-coordinated and some four coordinated. The reverse can also occur. The addition of water and heating can convert Lewis acid sites back to Brønsted acid sites. The aluminium atom is electrophilic and can react with a hydrocarbon to form an adsorbed carbenium ion (Charles *et al.*, 1991).

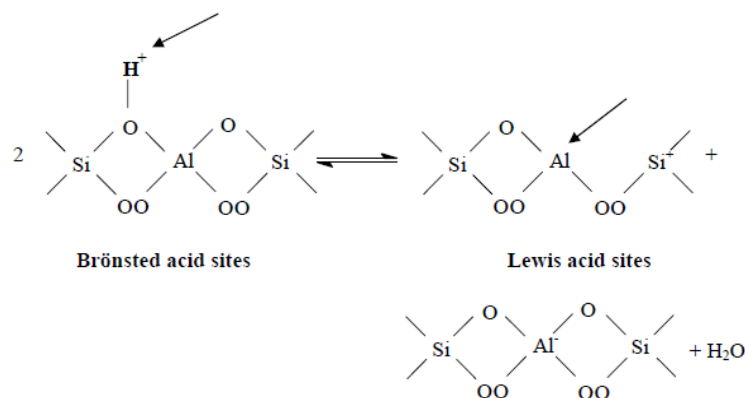


Fig 2.3 Brønsted and Lewis acid sites in zeolite framework

The catalytic activity of zeolites is determined by the strength of the acid sites. In general, the lower the aluminium content of a zeolite or the higher the Si/Al ratio, the

stronger the associated Brønsted acidity. Several characterization techniques have been developed to qualitatively and quantitatively estimate the acid sites and the relation between catalytic behaviour of zeolites and their acidity. The most widely used techniques are temperature programmed desorption (TPD) of ammonia, FTIR spectroscopy and catalytic testing in a reaction (Bagnasco *et al.*, 1996). The TPD of adsorbed NH₃ molecules is used to characterize the amount and strength of acid sites. Ammonia is the preferred adsorbing or desorbing gas because of its small size (kinetic diameter, 2.62Å) and its strong basicity (pK_b= 4.75). It can reach practically all the acid sites at the given temperature. Upon desorption at a programmed rate of temperature increase, NH₃ molecules will gradually desorb from the acid sites at various temperatures, depending on the strength of the acid sites. The latter aspect is exhibited by the profile of the NH₃ desorption curve. FTIR spectroscopy has been applied extensively to study the nature and the amount of acid sites present in a zeolite. Infrared spectroscopy (IR) has proven to be a valuable tool in characterizing hydroxyl species on the surface of molecular sieves and in measuring Brønsted and Lewis acidity (Szostak *et al.*, 1989).

2.3 ZEOLITE BETA

Zeolite Beta (IZA code, BEA) was first synthesized by (Wadlinger *et al.*, 1967). Zeolite beta represents the first high silica zeolite (Si/Al = 10-100) synthesized from a gel with alkali metal and an organic template, tetraethylammonium cations. BEA can be described by the general formula (Meier, *et al.* 1996): Na_n[Al_nSi_{64-n}O₁₂₈], where n = 7. The structure of BEA was described by Treacy *et al.*(1996) and Higgins *et al.* (1998). The first clues to the crystal structure of zeolite beta were evident from chemical and physical property measurements. Ion-exchange isotherms of Na-BEA at 25°C indicated that cations as large as tetraethylammonium ions, (TEA⁺) exchanged completely into the pore system. This behavior suggests that BEA contains at least 12 membered-ring channel openings, because TEA⁺ is too large to be exchanged through 10 membered-rings such as those in ZSM-5. The complete exchange of cations in BEA indicates the presence of channels instead of cages, because it is not possible to remove all the cations from cage structures such as Na-FAU. Zeolite Beta is an intergrowth hybrid of two distinct but closely related structures (polymorphs A and B) (Jansen *et al.*, 1997) which have tetragonal and monoclinic symmetry. In both systems, straight 12 membered-ring channels are present in two crystallographic directions perpendicular to [001] (Fig 2.4), while the 12 membered-ring in the third

direction, parallel to the c axis, is sinusoidal. The sinusoidal channels have circular openings (5.5 Å), and the straight channels have elliptical openings. The only difference between the two polymorphs (A and B) is in the pore dimension of the straight channels. In the tetragonal system, the straight channels have openings of 6.0 x 7.3 Å, whereas in the monoclinic system they are 6.8 x 7.3 Å. Figure 2.7 shows the BEA framework viewed along [100] and [001].

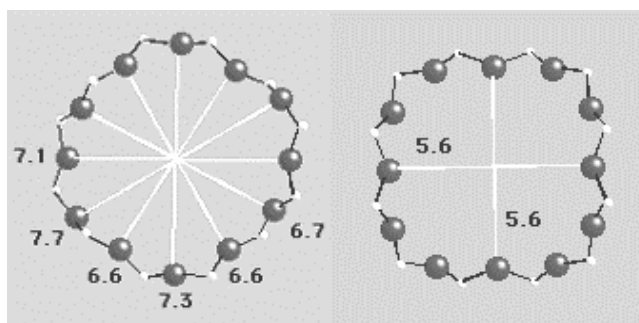


Fig 2.4 Zeolite beta framework viewed along a) [100], b) [001]

Zeolite beta is a potential acid catalyst due to the presence of large intersecting pores in a highly siliceous framework. It possesses high thermal and acid treatment stability, high strength of acid sites and is hydrophobic (Barrer, *et al.* 1982). Examples of successful applications of zeolite beta include aromatic alkylation of biphenyl with propylene (Aguilar *et al.*, 2000), aromatic acylation of 2-metoxynaphthalene (Casagrande *et al.*, 2000), indole synthesis, aromatic nitration and aliphatic alkylation. It is effective in lowering the pour point of petroleum oil by isomerizing the normal alkanes to their branched isomers, rather than cracking them to lighter alkanes, as is done by other zeolites such as ZSM-5 and erionite (Absil *et al.*, 1998). The shape selective catalytic properties of zeolite Beta, especially in the cracking of alkanes and in the isomerization of m -xylene, have also been investigated (Martens *et al.*, 1998; Corma *et al.*, 1989).

2.4 ZEOLITE CHARACTERIZATION TECHNIQUES

Knowledge of the structure, physical and chemical properties of zeolite catalysts is important to understand the chemistry occurring in catalysis. Characterization techniques were carried out to investigate the structure and properties of the zeolite beta catalysts. The catalyst sample was characterized using X-ray Powder Diffraction (XRD), Magic Angle Spinning Nuclear Magnetic Resonance (^{27}Al - MAS NMR), nitrogen adsorption and temperature programmed desorption (TPD) of ammonia.

2.4.1 X-ray Diffraction (XRD)

Zeolite materials, being crystalline solids have characteristic diffraction patterns that can be used to identify their exact structure and to determine their degree of crystallinity. The diffractions of X-rays from zeolite crystallites produce a scattering pattern which is specific of the periodic arrangement of regular arrays of atoms or ions located within the zeolite structure. Each zeolite has its own specific XRD pattern that can be used as reference for the solid crystal phase and as a fingerprint for the zeolite. This technique can also signify whether the solid sample is amorphous or crystalline. The purity of the solid crystal can be measured by comparing the XRD pattern of the sample with the XRD pattern of the standard sample.

For zeolite Beta, the determination of the degree of crystallinity is based on the intensity of the characteristic peaks at around $2\theta = 22.5^\circ$ (d_{302}). The degree of crystallinity calculated after background correction, is taken as the peak intensity of the zeolite sample divided by the peak intensity of the parent zeolite material that is taken as reference for 100% crystallinity. The degree of crystallinity is calculated using the following formula

$$\text{degree of crystallinity (\%)} = \frac{\text{Peak intensity of zeolite sample at peak } 2\theta = 22.5^\circ (d_{302})}{\text{Peak intensity of reference sample at peak } 2\theta = 22.5^\circ (d_{302})} \quad 2.1$$

2.4.2 Nitrogen Adsorption

The Braunauer-Emmett-Teller (BET) volumetric gas adsorption technique using N_2 or Ar is a standard method for the determination of the surface area and pore size distribution of finely divided porous samples (Brunauer *et al.*, 1938; Gregg and Sing, 1982). The relation between the amount adsorbed and the equilibrium pressure of the gas at constant temperature is defined as the adsorption (- desorption) isotherm. At least six different types of adsorption-desorption isotherms are recognized (Fig. 2.5).

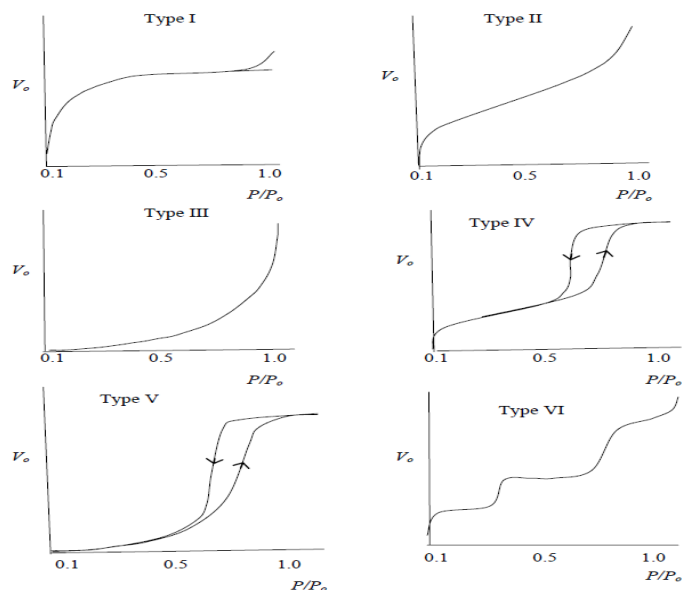


Fig 2.5 The six types of adsorption-desorption isotherms for microporous and mesoporous materials.

Typical type I isotherm always show high adsorption capacity and very fast saturation, followed by consistent adsorption over a wide range of p/p_o . These are characterized by high adsorption energies as in chemisorption. Nonporous (or possibly macro porous) materials with high adsorption energy exhibit adsorption isotherm of Type II while type III isotherm is for similar materials with low adsorption energies. Type IV isotherm is characteristic of mesoporous materials with high adsorption energy, while Type-V isotherms characterize similar materials with low adsorption energies. Type-VI are more difficult to assign and may arise due to many reasons, such as the presence of sites with distinctly different adsorption energies, pores of specific dimensions, ordering of the adsorbate molecules, etc.

Truly microporous materials like zeolites should exhibit Type-I isotherm, though, very often, these materials reveal Type-II or Type-IV isotherms depending on the size of the zeolite crystallites, presence of amorphous matter and meso porosity. The BEA samples examined in the present study revealed mainly Type-IV isotherms suggesting the presence of substantial amount of mesopores.

2.4.3 Temperature Programmed Desorption of Ammonia

Temperature programmed desorption (TPD) of ammonia was used to study the total surface acidity and the acid strength distribution of the acidic zeolite catalysts. The following assumptions are made regarding the adsorption and desorption of ammonia molecules:

- I. The intracrystalline zeolite surface is homogeneous and the amount of ammonia adsorbed in the experiment is less than that required for monolayer coverage,
- II. No readsorption of ammonia takes place during the desorption stage and
- III. There is no lateral interaction between the neighbouring adsorbed ammonia molecules.

The standard procedure for the TPD measurements involves the activation of the sample (50 – 200 mg) in flowing He or Ar at 873 K (3 h), cooling to 298 K, adsorbing NH₃ from a He (or Ar)-NH₃ (5 %) mixture, desorbing in He (Ar) at 373 K for 1 h, and finally carrying out the TPD experiment by raising the temperature of the catalyst in a linearly programmed manner (5 to 10 °C min⁻¹). The desorbed ammonia is measured by a thermal conductivity detector. The area under the TPD curves is converted into meq NH₃ per gram of catalyst based on injection of known volumes of the He (Ar)-NH₃ mixture under similar conditions. The NH₃-TPD thermogram profile obtained qualitatively shows the amount of ammonia desorbed at increasing temperature intervals which corresponds to the distribution of acid strengths of the total surface acidity.

2.4.4 Nuclear magnetic resonance (NMR)

High-resolution magic angle spinning nuclear magnetic resonance (NMR) spectroscopy in the solid state is a powerful complementary method to diffraction techniques for the investigation of zeolites and mesoporous molecular sieve structures (Bell *et al.*, 1994; van Bekkum *et al.*, 2001).

The main fields of application are: (i) Evaluation of the environment of the silicon framework atoms, (ii) framework n_{Si}/n_{Al} ratio of the mesoporous molecular sieves, (iii) silicon and aluminium ordering, (iv) identification of framework and non-framework aluminium, (v) incorporation of metals into mesoporous molecular sieves, (vi) determination of acidity of hydroxyl groups.

3. EXPERIMENTAL

3.1 CHEMICAL

The beta zeolite (Zeolyst International; CP814E), tetrapropylammonium hydroxide (TPAOH) (TCI Chemicals), sodium hydroxide (SRL Chemicals), nitric acid (Merck), cerium (III) nitrate (CDH chemicals), zinc nitrate hexahydrate (Merck), Iron (III) nitrate nonahydrate (Sigma Aldrich), tetra palladium chloride monohydrate (AR, Sigma Aldrich Chemicals), ruthenium trichloride hexahydrate (AR, Sigma Aldrich Chemicals), lauric acid (Loba Chemicals), anisole (Merck), acetophenone (Merck) and NaY(5.1) (Zeolyst International; CBV100) were used as procured.

3.2 INSTRUMENTS

X-ray diffraction (XRD) patterns for the calcined materials were obtained using a Rigaku Miniflex II with Cu K α irradiation. BET surface areas, t-plot analysis and pore volume measurements were carried out by N₂ adsorption (at liq. N₂ temperature) using a Micromeritics (ASAP 2010) instrument. The acidity of the catalysts was measured by the temperature-programmed desorption (TPD) of NH₃ (AutoChem 2910, Micromeritics, USA). The liquid product of the Friedel-Crafts acylation was analysed by gas chromatography (MICHRO 9100) using a FID detector and a BPX 70 (30m x 0.53mm) column. Product identification was done using ¹H NMR.

3.3 PREPARATION OF CATALYSTS

In this work, commercial zeolite beta (BEA) was modified to increase the activity in the acylation reaction. Metals like Pd and Ru were loaded on BEA and NaY(5.1) to study the hydrogenation of the ketone and anisole.

3.3.1 Modification of zeolite beta for acylation reaction

Commercial zeolite beta with SiO₂/Al₂O₃ ratio of 25 (SAR 25) code named BEA(25) was modified by three methods and used in the acylation of anisole with lauric acid:

1. Dealumination with nitric acid
2. Desilication with TPAOH, and
3. Ion-exchanging metal ions (Fe³⁺, Zn²⁺, Ce³⁺).

3.3.1.1 Dealumination procedure

Dealuminated samples of BEA were prepared from parent beta BEA(25). BEA(25) (5 g) was dealuminated by treating it with different concentrations of HNO₃ (60 g acid per g of zeolite) at two time intervals (1h and 6h) and at two temperatures (298 K and 358 K). The dealuminated samples were washed repeatedly with distilled water followed by dilute ammonia solution (6 wt%) to remove residual acid and free aluminium species. The samples were filtered and dried at 373 K for 6 h. All the samples were calcined in air at 723 K for 6h prior to use in the acylation reaction studies. Calcination temperature was increased slowly from room temperature to 723K. All the samples were characterized by XRD, to confirm the beta zeolite structure was maintained after dealumination. The samples obtained are referred to as BEA(58), BEA(88) and BEA(170), in which the number refers to the SiO₂/Al₂O₃ ratio of the sample. The conditions of preparation of the different dealuminated samples are presented in Table 3.1.

TABLE 3.1 Conditions used in the dealumination of beta

Sample code	Conc of nitric acid	Temperature	Time (h)
Parent BEA(25)	-	-	-
BEA(58)	10 %	298 K	1
BEA(88)	10 %	298 K	6
BEA(170)	55%	358 K	6

3.3.1.2 Desilication procedure

While acid treatment removes Al specie (from framework and other positions), alkali treatment removes Si (desilication). Alkaline treatment was carried out in a round bottom flask with different volume (30 and 20ml) of 0.5 M aqueous solution of tetrapropylammonium hydroxide (TPAOH) at two different temperatures (333 K and 343 K). BEA(25) (2 g) was added to a continuously stirred mixture of TPAOH kept at the required temperature. The mixture was treated for 4 h and the resulting sample was washed with distilled water until pH neutral, filtered, dried at 373 K for 12 h, and calcined at 723 K for 4h. The samples are referred as BEA(DS1) and BEA(DS2). The condition employed to prepare these samples are given in Table 3.2.

Table 3.2 Conditions of desilication

Sample code	Conc of TPAOH acid	Temperature	Time (h)
Parent BEA(25)	-	-	-
BEA(DS1)	30 ml (0.5 M)	343 K	4
BEA(DS2)	20 ml (0.5 M)	333 K	4

3.3.1.3 Preparation of the Ion- exchange beta zeolites

The parent zeolite was ion-exchanged with different salt ((Fe³⁺ nitrate, Zn²⁺ nitrate, Ce³⁺ nitrate) solutions to yield metal loaded samples. The procedures adopted are expected to lead to metal loading of about 2 wt%. Separate analysis of the metal content was not carried out.

3.3.1.3.1 Ion-exchange of BEA(25) with Fe³⁺ ions:

A mixture containing 5g BEA (25) and 144ml of 0.0125M iron (III) nitrate solution was stirred at 353K for 24h. Then the zeolite was recovered by filtration and washed repeatedly with distilled water. The sample was dried for 12h at 393 K, and calcined at 723 K for 4h.

3.3.1.3.2 Ion-exchange of BEA(25) with Zn²⁺ ions:

BEA(25) (5g) was stirred with 120ml of 0.0125M zinc nitrate solution at 353K for 24h. Then the zeolite was recovered by filtration and washed repeatedly with distilled water. The sample was dried for 12h at 393 K, and calcined at 723 K for 4h.

3.3.1.3.3 Ion-exchanging of BEA(25) with Ce³⁺ ions:

The mixture containing 5g BEA (25) and 100 ml of 0.007M cerium (III) nitrate solution was refluxed at 353K for 24h. Then the zeolite was recovered by filtration and washed repeatedly with distilled water. The sample was dried for 12h at 393 K, and calcined at 723 K for 4h.

3.3.2 Catalyst preparation for hydrogenation reaction

Pd, Pt, Ru and Ni are used often for the hydrogenation of organic compounds. In this study, hydrogenation of anisole and acetophenone was done using Pd and Ru supported on an acidic support (BEA(58)) and a basic support (NaY(5.1)). The supports were loaded with the metal salts by a wet impregnation procedure.

3.3.2.1 Impregnation with Pd:

Palladium was loaded on BEA(58) by a wet impregnation method using a solution of $(\text{Pd}(\text{NH}_3)_4 \text{Cl}_2)$. The required amount of the salt (to yield 0.5 wt% Pd loading) was dissolved in 5 mL of water, followed by the addition of 1.5 g of BEA(58). The mixture was stirred for 1 h at 30 °C. The impregnated sample thus obtained was dried overnight at 100°C. Finally, the Pd salt loaded BEA (58) was calcined at 400°C for 4 h.

A similar procedure was used to load 0.5% Pd on NaY(5.1).

3.3.2.2 Impregnation with Ru:

RuCl_3 was used as the source of Ru species. RuCl_3 was dissolved in 5 mL of water, followed by the addition of 1.5 g of BEA(58). The mixture was stirred for 1 h at 30 °C. The impregnated sample thus obtained was dried overnight at 100°C. Finally, it was calcined at 400°C for 4 h. The amount of RuCl_3 taken was calculated to produce a loading of 0.5 wt % of Ru.

3.3 CHARACTERIZATION TECHNIQUES

A number of techniques were used to characterize the catalysts used in these studies.

3.3.1 X-ray Diffraction

The samples were characterized by X-ray diffraction in order to confirm the phase structure, crystallinity and the purity of the zeolite. XRD patterns were acquired on a Rigaku Miniflex II with Cu $K\alpha$ irradiation using CuK_α radiation with $\lambda = 1.5406 \text{ \AA}$ at 40 kV and 10 mA. The sample was carefully ground to a fine powder, and then lightly pressed between two glass slides to get a thin layer. X-ray diffractograms were obtained in the range of 2θ from 2° to 80°. Scanning was carried out in step intervals of 0.05° 2θ with a counting time of 1 second per step. X-ray diffractograms obtained from modified BEA and metal loaded zeolites was compared with the diffractograms of the parent zeolites. The intensity of the peak at $2\theta = 22.4^\circ\text{-}22.6^\circ$ was used to determine the crystallinity of the BEA samples giving a crystallinity value of 100% to the parent zeolite [BEA(25)].

3.3.2 Solid State NMR Spectroscopy

The solid state ^{27}Al MAS n.m.r. spectra were recorded at ambient temperature using a Bruker MSL-300 FT- n.m.r. spectrometer. Three thousand FIDs were accumulated before FT to obtain spectra with good S/N ratios. A 5 s delay time was

used between each 90^0 pulse. An aqueous solution of AlCl_3 provided the reference peak for $^{27}\text{AlMAS}$.

3.3.3 Nitrogen Adsorption

BET surface areas of zeolite Beta samples were analyzed using nitrogen adsorption technique. Nitrogen was used as an adsorbate at 77 K. Before measurement was performed, about 0.2 g of the sample was dehydrated at 200°C for 3 hours. The dehydrated sample was weighed accurately and the samples were then evacuated to 10^{-2} Torr and immersed in liquid nitrogen. The surface areas and pore volumes of the sample were calculated automatically by the instrument from nitrogen adsorption data.

3.3.4 Temperature programmed desorption (TPD) of NH_3

Ammonia (NH_3) gas was used as the adsorbate. The standard procedure for the TPD measurements involved the activation of the sample in flowing He at 873K (1 h), cooling to 323K, adsorbing NH_3 from a He- NH_3 (10 %) mixture, desorbing He at 323K for 30 min, and finally carrying out the TPD experiment by raising the temperature of the catalyst in a programmed manner (10 K min^{-1}). The areas under the TPD curves were converted into meq NH_3 desorbed per gram of catalyst based on injection of known volumes of the He- NH_3 mixture under similar conditions.

3.4 CATALYTIC TEST

Dealuminated, desilicated and metal loaded (Fe, Zn, Ce) samples were tested for the acylation reaction while Pd, Ru metal loaded samples were tested for the hydrogenation reactions.

3.4.1 Acylation of Anisole with lauric acid over BEA catalysts

Most of the reactions were carried out using a glass batch reactor. The freshly prepared catalyst (0.5 g) was immediately placed in a 50 mL two necked round bottle flask equipped with a reflux condenser containing a mixture of anisole (0.2mol) and lauric acid (0.0025 mol). The reaction mixture was stirred and heated at 155°C for 30 hours. The round bottle flask was kept in an oil bath with a magnetic stirrer as shown in Figure 3.1. The liquid product was syringed out at the intervals of 3, 6, 9, 12, 15, 18, 21, 24, 27 and 30 h. The liquid product obtained was separated from suspended catalyst powder and placed in glass vials for further characterization using GC. Some of reactions were done in a Parr reactor (100 ml) using the same conditions, i.e. 155°C and atmospheric pressure especially to study the effect of agitation (200, 300, 400,

500, and 600 RPM). The reaction products were analysed and the reaction path has been illustrated in the scheme 1(fig 3.2).

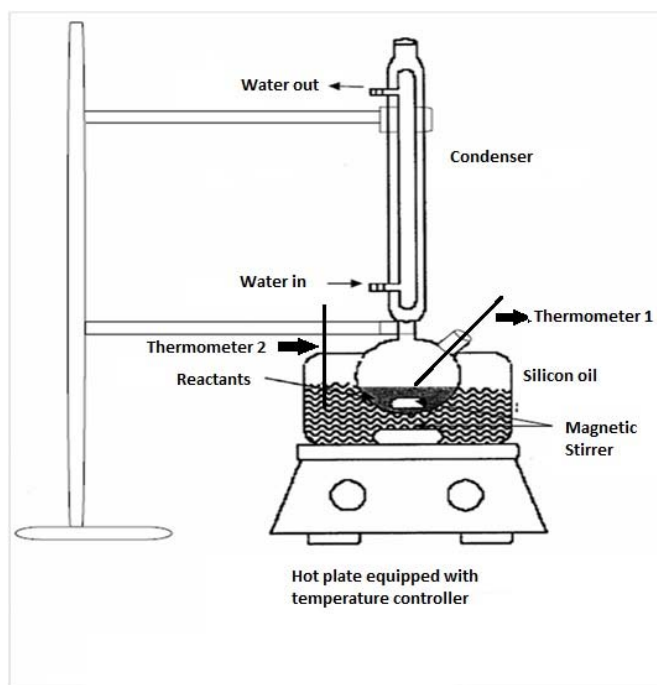


Fig 3.1 Pictorial representation of the batch reactor used

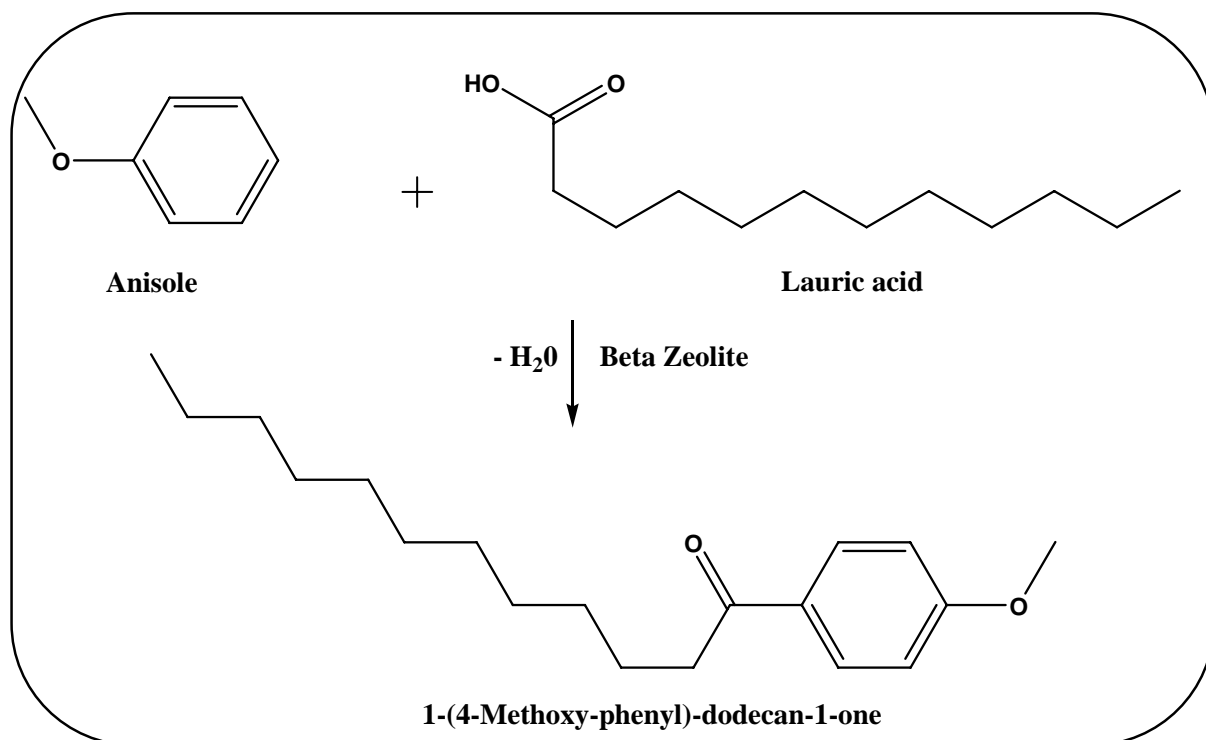


Fig 3.2 Scheme for the acylation of anisole with lauric acid

3.4.2 Product identification

Products were identified by injecting standards for phenol and methanol, while the ketone was identified by ^1H NMR. The pure ketone was obtained from the reaction mixture by the following procedure: the catalyst was separated from the reaction mixture by filtration and dissolved in ether, the acid and phenol were removed from the reaction mixture by extraction with sodium hydroxide. The organic layer was separated. Diethyl ether was removed by evaporation, while anisole was removed by distillation. Finally the product was purified by column chromatographic using SiO_2 gel 100-200 mesh and chloroform.

3.4.3 Hydrogenation of anisole and acetophenone

Hydrogenation reactions were carried out in a Parr reactor (100 ml). Hydrogenation of anisole and acetophenone was done at 155 °C and 25 bar H_2 pressure in the presence of Pd/ BEA(58), Pd/NaY(5.1) and Ru/BEA(58). All the catalysts were reduced in H_2 atmosphere for 400 °C for 4 h before the reaction. The catalysts were reduced in a tubular furnace and cooled in hydrogen followed by N_2 flushing. The reduced sample kept in a boat was quickly transferred to the Parr reactor and the hydrogenation was carried out. At the end of the reaction, the reaction mixture was filtered off to remove the catalyst. The products were analyzed in gas chromatograph.

4. RESULTS AND DISCUSSION

A. ACYLATION OF ANISOLE WITH LAURIC ACID

4.1 PHYSICOCHEMICAL CHARACTERIZATION OF BEA SAMPLES

The parent zeolite beta (CP814E, Zeolyst International) and its various modifications were characterized by a number of methods, such as XRF analysis for determining $\text{SiO}_2/\text{Al}_2\text{O}_3$ ratio, XRD, N_2 adsorption-desorption isotherms for textural characterization and TPD of NH_3 for acidity measurement. The results of these characterization studies are presented in this section.

4.1.1 Compositional analysis of the samples

As the acylation reaction is an acid catalyzed reaction, it was decided to study the effects of altering the Al-content ($\text{SiO}_2/\text{Al}_2\text{O}_3$ ratio) of the parent zeolite on its activity. This was carried out by i) dealumination with HNO_3 (to decrease Al-content; increase $\text{SiO}_2/\text{Al}_2\text{O}_3$ ratio) and ii) desilication with TPAOH (to increase Al-content; decrease $\text{SiO}_2/\text{Al}_2\text{O}_3$ ratio). The $\text{SiO}_2/\text{Al}_2\text{O}_3$ ratios of the zeolite after the dealumination and desilication treatments obtained from XRF analysis, are presented in Table 4.1. It is noticed that increasing the temperature of dealumination or increasing the acid (HNO_3) increases dealumination, nearly 85 % of all the Al being removed from the parent sample after treatment #4. Similarly, increasing the temperature of the alkali (TPAOH) treatment increases desilication

Table 4.1 Compositional analysis by XRF spectroscopy

#	Sample code	Sample	SAR [SiO ₂ / Al ₂ O ₃]	Metal [wt %]
1	BEA(25)	BEA (parent sample)	25	-
2	BEA(58)	Dealuminated-10%HNO ₃ RT	58	-
3	BEA(88)	Dealuminated-25%HNO ₃ 85°C	83	-
4	BEA(170)	Dealuminated-55%HNO ₃ 85°C	170	-
5	BEA(DS1)	Desilicated at 70 °C	(22)	-
6	BEA(DS2)	Desilicated at 60 °C	(21)	-
7	BEA-Fe	Fe ³⁺ -exchanged BEA (25)	25	(2)
8	BEA-Zn	Zn ²⁺ -exchanged BEA (25)	25	(2)
9	BEA-Ce	Ce ³⁺ -exchanged BEA (25)	25	(2)

Values in parentheses, (), are estimated values based on earlier work and metal content of solutions used for ion-exchanging.

4.1.2 XRD studies of the modified BEA samples

The XRD patterns of the different modified BEA samples are presented and discussed in this section.

a. Dealuminated samples

Figure 4.2.1 presents the XRD patterns of dealuminated samples calcined at 450 °C. The XRD pattern of the samples did reveal small changes in the patterns, such as a minor shift of the d₃₀₂ line towards higher 2θ values (Table 4.2) compared to that of the parent zeolite BEA (25) and some loss in intensity of the peaks. The shift in the d₃₀₂ line towards higher 2θ values is due to removal of Al³⁺ ions from the framework and consequent decrease in unit cell dimensions. The loss in intensity of the lines is due to partial destruction of the zeolite lattice (crystallinity loss) on removal of the frame work Al-ions.

The crystallinity loss of the samples was calculated by comparing the intensity of the most intense peak (d₃₀₂) of the dealuminated sample relative to that of BEA (25) assuming 100 % crystallinity for the parent zeolite. Relative crystallinities of the dealuminated samples are presented in Table 4.2. It is noticed that increasing dealumination increases crystallinity loss and severe dealumination (55 % HNO₃ at 85 °C; SAR = 170) causes severe (50 %) loss in crystallinity.

TABLE 4.2 Relative crystallinities of the parent and dealuminated samples

Sample code	% Al-ions removed	d_{302} (degrees, 2θ)	Relative crystallinity (%)
SAR(25)	0	22.5	100
SAR(58)	57	22.7	90.6
SAR(88)	72	22.9	84.3
SAR(170)	85	23.0	50

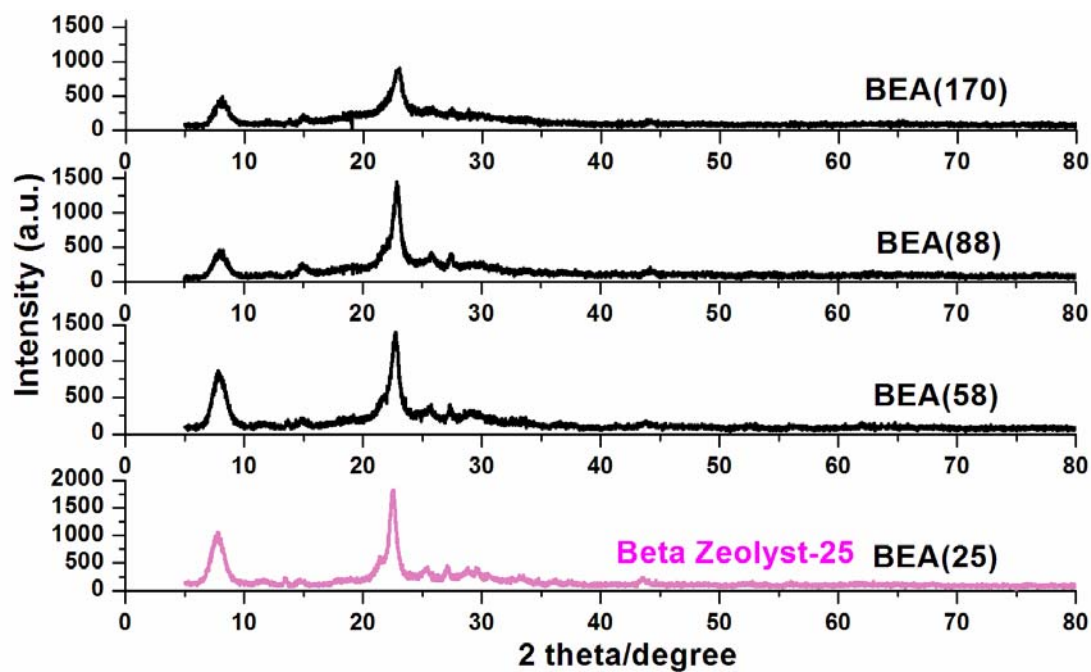


Fig 4.1 XRD patterns of the dealuminated samples and the parent zeolite

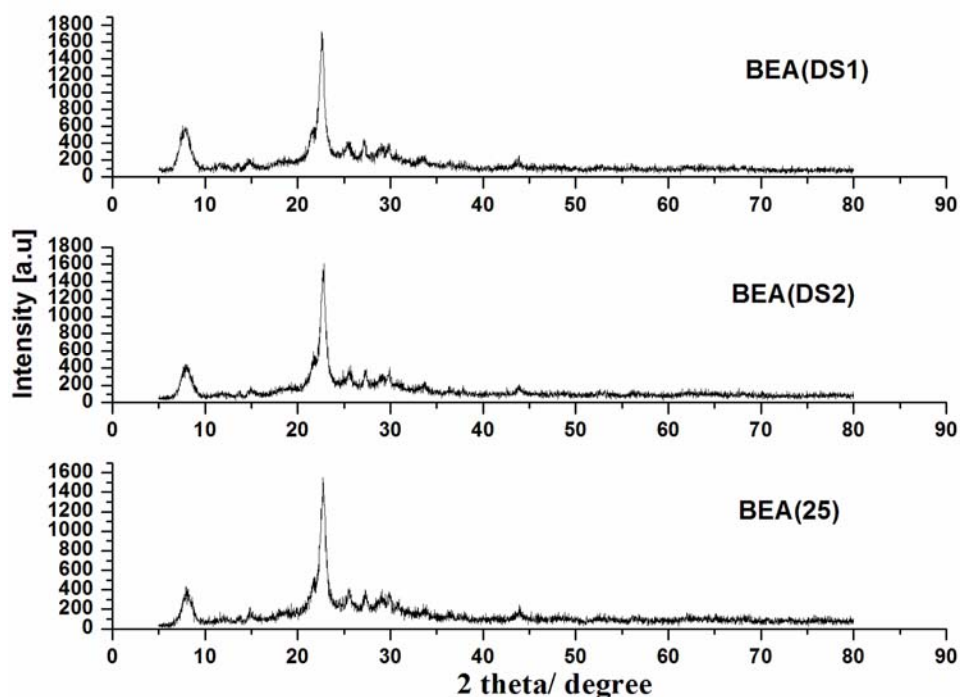


Fig 4.2 XRD patterns of the desilicated samples and parent zeolite

b. Desilicated samples

The XRD patterns of two BEA samples desilicated with TPAOH are presented in Fig. 4.2. The patterns do not reveal significant changes in peak intensities or peak positions. This is due to the mild nature of the desilication process and the relatively small amounts of Si removed from the framework.

c. Metal exchanged samples

Fe^{3+} , Zn^{2+} and Ce^{3+} ions were loaded in the BEA samples by ion-exchange procedure. The amount of metal ions used during ion-exchange was expected to lead to a loading level of about 2 wt% of the metal. The exact quantity of the metal could not be estimated accurately. The XRD patterns of the metal ion loaded BEA samples are presented in Fig. 4.3. The XRD patterns do not reveal any additional peaks attributed to metal oxides, presumably due to the small loading and their presence as ions in exchange positions in the zeolite. However, the intensities of the peaks are slightly decreased on loading of the metal ions. This is generally observed when large metal ions are loaded in zeolites.

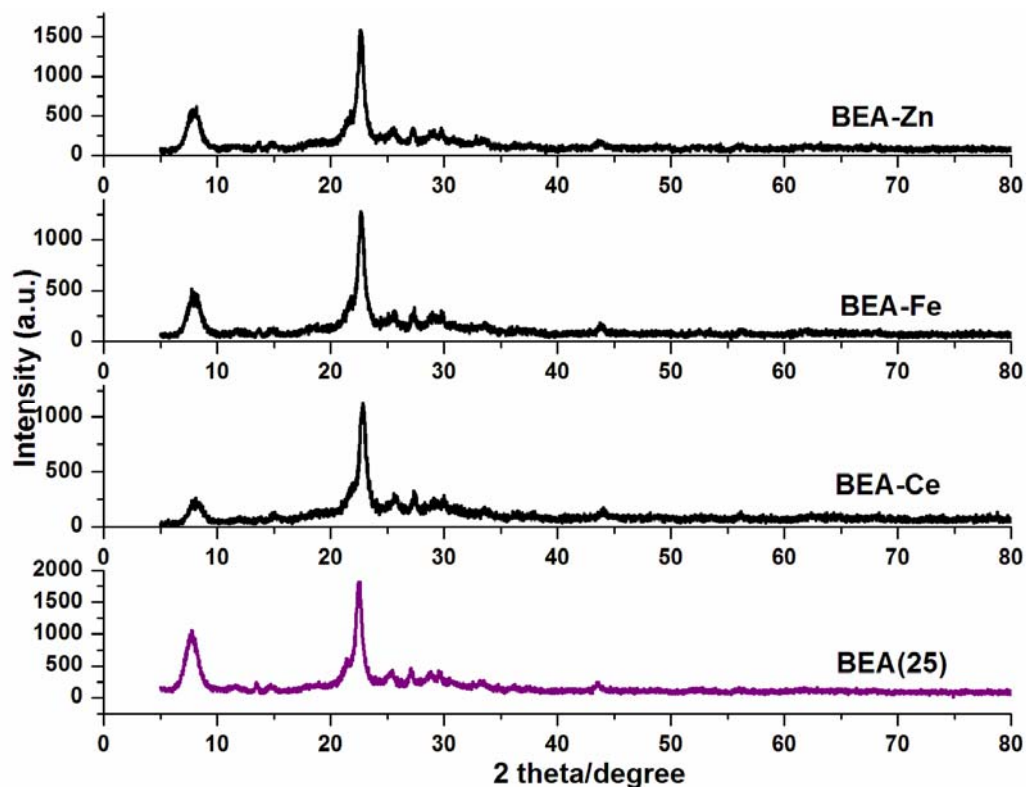


Fig 4.3 XRD patterns for metal loaded BEA samples and parent BEA

4.1.3 Surface areas and pore volumes by N₂ sorption:

Nitrogen adsorption isotherms of the different BEA samples were obtained at liq. N₂ temperature in order calculate surface areas and pore volumes. The adsorption isotherms of the different samples were typically of Type-IVA with a Type-I feature at lower p/p_o values suggesting the presence of both micro and mesopores. A typical adsorption-desorption isotherm, that of the parent BEA, is presented in Fig. 4.4.

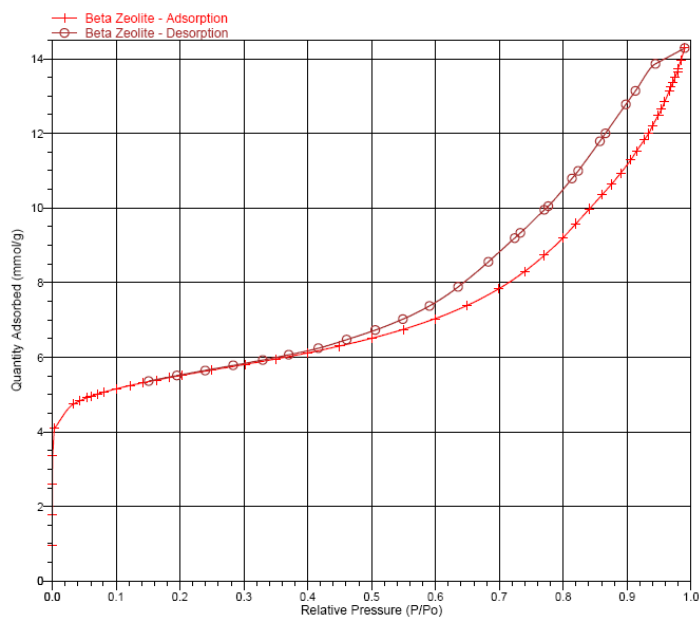


Fig. 4.4 Adsorption-desorption isotherms of parent BEA

The isotherms were analyzed using the BET and t-plot methods. The results of the analyses are presented in Table 4.1.3. Though the BET equation is not exactly applicable for microporous zeolites, it is now being used in our studies for convenience in comparison and due to the fact that substantial amount of mesoporous area is present in the samples. It is seen from the table that the parent zeolite possesses substantial amounts of external surface, presumably from the external surface area contribution by the small zeolite crystallites and mesoporous present in the zeolite crystallites and amorphous material present in the samples. S_{BET} (column #2) decreases on dealumination, while it increases slightly on desilication. Interestingly, S_{ext} (column #4) decreases after both treatments, while S_{micro} (column #3) increases with mild dealumination (to SAR = 58) and decreases with strong dealumination treatments; S_{micro} increases on desilication. The decrease in the S_{ext} is essentially due to the dissolution of amorphous material. The increase in the S_{micro} on mild dealumination and desilication (essentially, mild treatments) is due to the removal of the debris (Si- and Al-specie) from the pore system and making the pores more accessible to N_2 molecules. This argument is supported by the slight increase in the micropore volume (column #6) noticed on mild dealumination and desilication.

Interestingly, the total pore volume (column #5) increases with both treatments; the increase appears to be mainly due to the increase in the mesopore volume (column #7). The average diameter of the pores associated with the mesopore area was calculated using the equation:

$$d = \frac{4 * vol_{meso}}{Area_{meso}} \quad (4.1.1)$$

This calculation assumes that S_{ext} arises only from the pores and ignores contributions (expected to be small) from the external surface of zeolite crystallites. The calculations reveal that the average pore diameter of the mesopores (column #8) increases substantially on both dealumination and desilication. This increase is probably due creation of new mesopores inside the zeolite crystallites and fusion of smaller pores into larger pores.

Table 4.3 Surface area and pore volume of the dealuminated and desilicated BEA samples

Sample code	Surface Area (m ² /g)						Mesopore dia. (Å) ^c
	BET			t-plot			
	BET	t-plot	External area (meso) ^a	total	t-plot (micro-pore)	meso-pore ^b	
<i>(Column #)</i>	<i>2</i>	<i>3</i>	<i>4</i>	<i>5</i>	<i>6</i>	<i>7</i>	<i>8</i>
BEA(25)	413	237	176	0.50	0.11	0.39	88
BEA(58)	427	269	158	0.74	0.13	0.61	153
BEA(88)	354	221	133	0.75	0.11	0.64	192
BEA(170)	302	160	142	0.73	0.08	0.65	184
BEA(DS1)	436	285	151	0.78	0.14	0.65	172
BEA(DS2)	425	289	136	0.78	0.14	0.64	188

^a: ($S_{BET} - t\text{-plot micropore area}$); ^b: (total pore volume – t-plot micropore volume);

^c: ($4V_{mesopore} / S_{mesopore}$)

4.1.4 Acidity of dealuminated samples from TPD of NH₃

The acidity of the dealuminated BEA samples was determined by the TPD of NH₃. The results are presented in Table 4.1.4. As the number of acid sites (total acidity) in a zeolite depends upon its Al content (one acid site per Al atom), a

reduction in acidity is expected to occur on dealumination. This is found to be so in the case of the dealuminated BEA samples (Table 4.4). However, as seen from the table, the amount (mmole) of NH₃ desorbed is much more than the amount (mmole) of Al present in the samples. This is because the total amount of NH₃ desorbed has been calculated from the total area under the desorption curve and this includes physically adsorbed NH₃ also. Though TPD measurements cannot identify the nature or type (Lewis or Brönsted), Marques *et al.* (2003) have reported the presence of equal amounts of Lewis and Brönsted sites in the same commercial sample used by us (CP814E supplied by Zeolyst).

Table 4.4 Acidity of dealuminated BEA from TPD of NH₃

Sample	SAR (SiO ₂ /Al ₂ O ₃)	Al (mmol / g)	Acidity (mmol NH ₃) /g
BEA(25)	25	1.2	3.1
BEA(58)	58	0.6	2.6
BEA(88)	83	0.9	2.1
BEA(170)	170	0.2	1.2

4.1.5 ²⁷Al MAS-NMR spectrum of BEA (25)

The ²⁷Al MAS NMR spectra of the parent zeolite (BEA(25)) is presented in Fig. 4.5. ²⁷Al NMR characterization of zeolites can reveal the nature of the Al-specie, especially the presence or absence of extra-framework (non Td) Al-specie. In the case of the present sample, though the majority of the Al is in Td coordination (52.8 ppm; mostly in the framework), a significant amount of Al is found to be present in Oh coordination ($\delta \sim 0$ ppm) also, suggesting the presence of extra framework Al and probably amorphous material also.

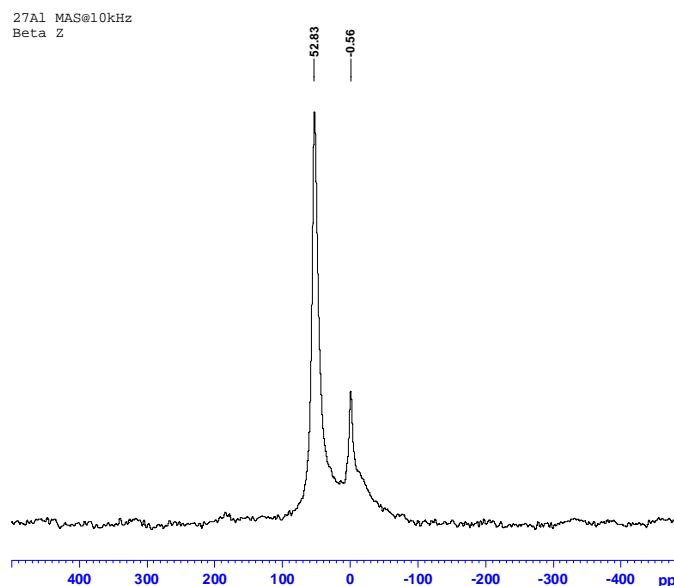


Fig. 4.5. ^{27}Al spectra of the parent BEA used in the studies

4.2. Catalytic Activity of Zeolite Beta in Friedel-Crafts Acylation

Friedel-Crafts acylation of anisole with lauric acid has been carried out over the different samples of BEA using a batch reactor. The effects of various reaction parameters, such as run duration, temperature, mole ratio of the reactants (anisole : lauric acid) and stirring speed were investigated. The products were analyzed by gas chromatographic methods. Separation of the major compound (acylated product, ketone) from the reaction mixture was done by distillation and elution using a chromatographic column. Identification of the ketone was done by its NMR spectra. All the conversions reported in this section have been calculated based on lauric acid. The product distributions reported have been calculated based on GC area as some of the compounds (listed as others) were unidentified and standard samples for these could not be obtained to establish GC response factors for all the compounds.

4.2.1 Influence of changing the $\text{SiO}_2/\text{Al}_2\text{O}_3$ ratio through dealumination and desilication methods

The acylation of anisole with lauric acid was carried out using BEA samples obtained after dealumination and desilication treatments. The results from these studies are discussed below.

a. Effect of dealumination

The activity of the parent BEA and the different dealuminated samples are

presented in Fig.4.6 and in Table.4.5. The conversions obtained over these samples at various run durations are presented in the figure. At the end of 30 hours, the conversions over the catalysts are as follows: 38 % for BEA (25), 52 % for BEA(58), 11% for BEA (88) and 4 % for BEA(170). The activity of the catalysts decreases in the order, BEA(58) > BEA(25) > BEA(88) > BEA(170). It is noticed that the moderately dealuminated sample BEA(58) is more active than the parent zeolite BEA(25), while the more extensively dealuminated samples, BEA (88) and BEA(170) are less active. Examining the product distribution, the major product is found to be the ketone, all the three isomers (o-, m-, and p-) being present in the product. The amount of the three isomers in the product is in the decreasing order, p- > o- . m-. The m-isomer is the least formed in the reaction even though it is thermodynamically the most stable one suggesting that the reaction is kinetically controlled. Small amounts of methanol and phenol are also found to be formed through cleavage of the ether (-O--Me bond) in anisole.

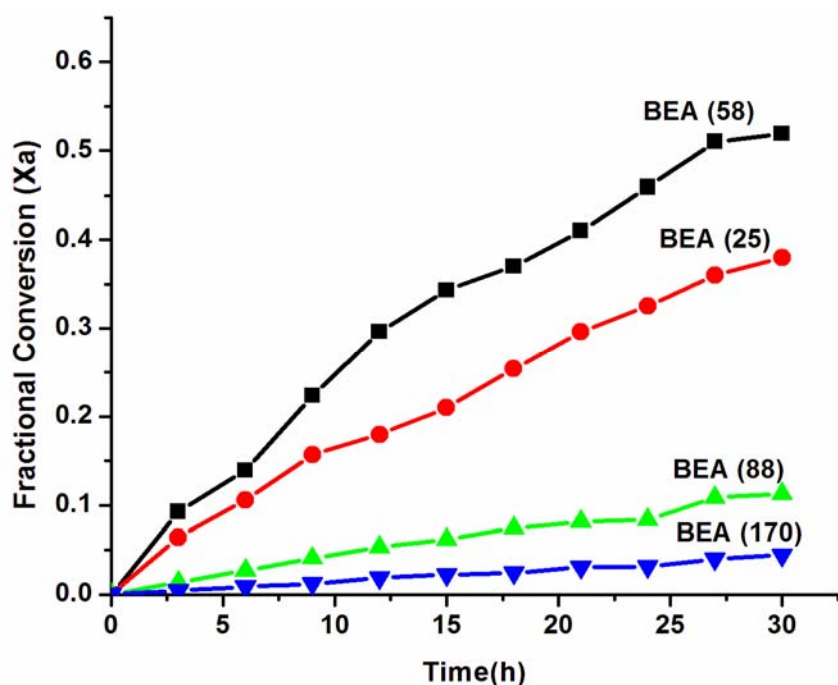


Fig.4.6 Effect of dealumination on acylation reaction

Anisole: C₁₂ acid = 8:1 (mole); Temp = 155 °C; C₁₂: Catalyst = 10:1 (Wt.)

When dealumination is done, acidity decreases due to loss of both framework Al and extra-framework Al-specie (Table 4.4) and one would therefore, expect catalytic activity to decrease. This found to be so when strong dealumination is done; both BEA(88) and BEA(170) possess lower activity than the parent zeolite, BEA(25)

(Table 4.5). However, in the case of the mildly dealuminated catalyst [BEA(58)], the activity is found to be much higher. This increase in activity with SAR (or decreasing acidity) on mild dealumination is surprising. This increase can be attributed to the creation of mesopores in the dealuminated samples and the ease of diffusion of the reactants and products. Ma. *et al.* have reported a similar trend during the acylation of anisole with propionic acid in a batch reactor in the absence of a solvent over FAU samples with different Si/Al ratios. They have attributed the increase in activity on dealumination to the creation of Lewis acid centers. Freese *et al.* also reported an increase in the initial activity of BEA (Si/ Al = 12) on dealumination (to Si/Al = 90) and attributed it to the creation of mesopores and increased mass transfer in the dealuminated sample.

Table 4.5 Product distribution for acylation reaction on different modified BEA samples

Samples (SAR)	Product distribution (area %)						Conversion (mole %)
	Ketone			MeOH	phenol	Others	
	<i>para</i>	<i>ortho</i>	<i>meta</i>				
BEA(25)	63.2	12.4	0.2	2.2	4.6	17.2	38.1
BEA(58)	70.1	8.9	1.3	0.4	4.3	15.0	51.9
BEA(88)	54.4	11.4	5.3	0.7	4.9	23.3	11.3
BEA(170)	57.5	9.8	7.0	1.3	7.5	16.9	4.4
BEA(DS1)	61.5	11.2	1.4	0.2	5.1	20.5	53.6
BEA(DS2)	57.2	9.5	0.9	0.3	5.1	27.0	48.1
BEA-Fe	75.4	9.2	-	0.9	4.3	9.8	67.0
BEA-Zn	73.5	11.7	0.6	0.5	1.9	11.8	72.1
BEA-Ce	62.9	13.6	0.5	1.6	5.4	16.0	59.0

(Anisole: C₁₂ acid = 8:1 (mole); Temp = 155 °C; C₁₂: Catalyst = 10:1 (wt.); Run duration = 30 h)

It is likely that the increase in the activity of the zeolites on mild dealumination in our case is also due primarily to the creation of mesopores that cause an increase in

mass transfer. N₂ sorption studies have revealed an increase in total pore volume and an increase in the average pore diameter of the samples on dealumination (Table 4.3). Further, the increase in the micropore volume (from 0.11 cm³/g for BEA(25) to 0.14 cm³/g for BEA(58)) for the mildly dealuminated sample suggests that a larger amount of zeolitic pores will be available for the reaction. In the case of the other two (highly dealuminated) samples, the micropore volumes are lower revealing destruction of the zeolite structure. The lower activity of these two samples [BEA(88) and BEA(170)] in spite of larger mesopore diameters is a result of their lower acidities.

b. Effect of desilication:

The influence of desilication on activity and product distribution are presented in Fig. 4.7 and Table 4.5, respectively. Desilication increases conversion from 38% for the parent zeolite [BEA(25)] to 54 % for BEA (DS1) and 48% for BEA (DS2). Over these samples also, the p-isomer of the ketone is the most favoured product. The increase in activity on desilication is also attributed to the creation of larger mesopores and greater access of the micropores for the reaction (Table 4.3). Very similar results have been reported by Matias *et al.*, (2011) who have investigated the influence of desilication with NaOH on the activity of ZSM-22 (TON) in the isomerization of 1-butene. These authors have also observed an increase in mesopore volume and the opening of zeolite micropores on treatment with NaOH.

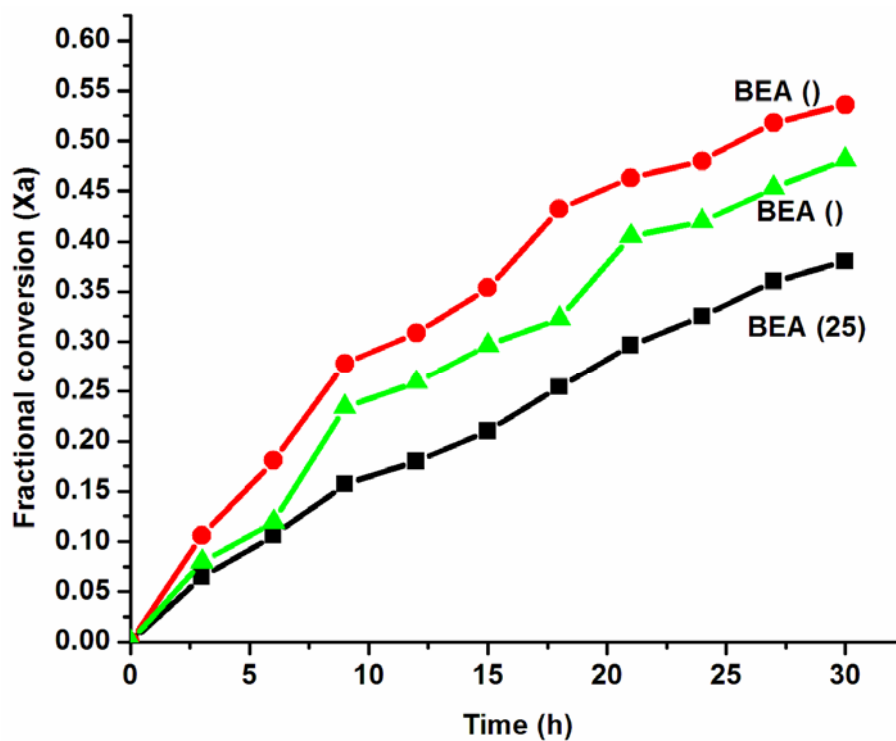


Figure 4.7 Effect of desilication on acylation reaction

Anisole: C₁₂ acid = 8:1 (mole); Temp = 155 °C; C₁₂: Catalyst = 10:1 (wt)

4.2.2 Effect of ion-exchanging with cations

Beta Zeolite BEA (25) was loaded with Ce³⁺, Zn²⁺ and Fe³⁺ ions by ion-exchanging and the activities of the metal loaded catalysts were examined for the acylation reaction (Fig 4.8 and Table 4.5). The order of activity is found to be BEA-Zn > BEA-Fe > BEA-Ce > BEA(25).

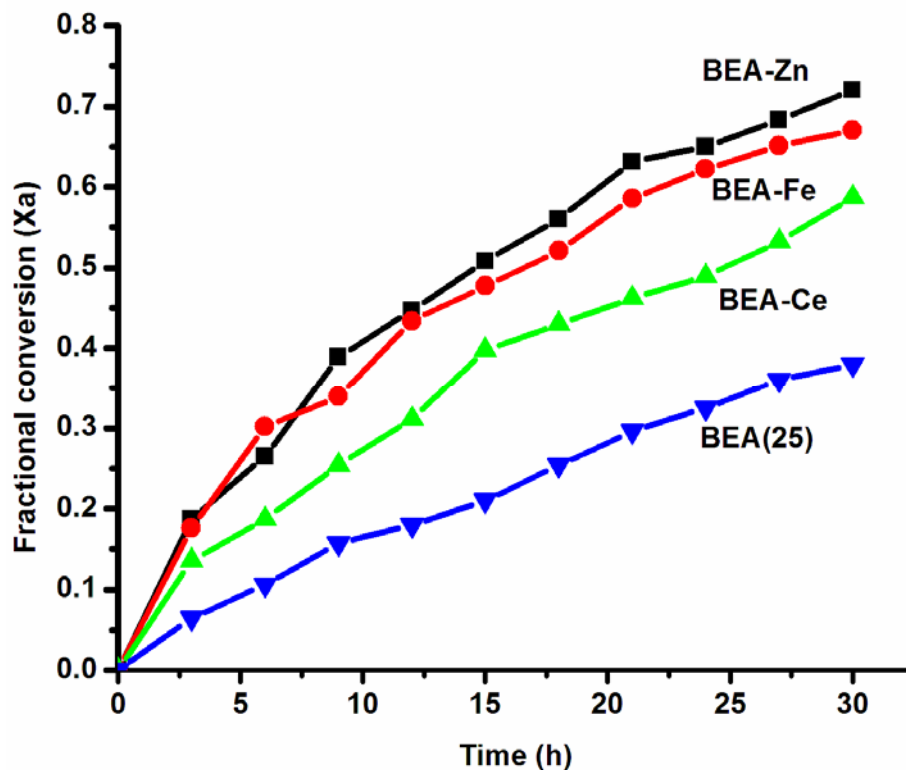


Figure 4.8 Effect of metal ion-exchange with cation on acylation reaction

Anisole: C₁₂ acid = 8:1 (mole); Temp = 155 ° C; C₁₂: Catalyst = 10:1 (wt)

The increase in conversion on metal loading is probably due to an increase in acidity. Additional acid sites could be created when multivalent ions are exchanged in zeolites through hydrolysis reactions as shown below.



Besides, the cations themselves can act as weak Lewis acid sites catalyzing the reaction. Earlier workers (Boyapati *et al.*) have also reported similar results. They studied the acylation of aromatic ethers with acetic anhydride in the presence of montmorillonite exchanged with different cations (Fe³⁺, Zn²⁺, Cu²⁺, Al³⁺ and Co²⁺) and found the Fe³⁺ and Zn²⁺ exchanged samples to be the most active. In these studies, one aspect that needs to be investigated is the leaching of the cations into solution during the reaction and their possible catalytic activity.

4.2.3 Effect of External Mass Transfer

This is a typical solid-liquid slurry reaction involving the transfer of lauric acid (A) and anisole (B) to the catalyst where in external mass transfer of reactants to the surface of the catalyst particle, followed by intraparticle diffusion, adsorption, surface reaction, and desorption, takes place. The influence of external solid-liquid mass-transfer resistance must be ascertained before a true kinetic model could be developed. Thus, experimental and theoretical analyses were done. The reaction studied in this case involves two reactants in organic phase, which react on the surface of the catalyst to form liquid-phase (organic) products at the chosen reaction temperature. The overall reaction can be represented as follows:



Where, A and B are the reactants and D and E are the products and z is the stoichiometric coefficient of B. At steady state, the rate of mass transfer per unit volume of the liquid phase ($\text{kmol}/\text{m}^3\text{s}$) is given by:

$$r_a = k_a a_p ([A_0] - [A_s]) \quad (4.2.2.2)$$

(rate of transfer of A from bulk liquid to external surface of the catalysts particle)

$$r_a = z k_b a_p ([B_0] - [B_s]) \quad (4.2.2.3)$$

(rate of transfer of B from bulk liquid to external surface of the catalysts particle)

$$= r_{\text{obs}} \quad (4.2.2.4)$$

= rate of reaction within the catalysts particle.

When the external mass transfer resistance is small, then the following inequality holds,

$$\frac{1}{r_{\text{obs}}} \gg \frac{1}{k_a a_p [A_0]} \text{ and } \frac{1}{k_b a_p [B_0]} \quad (4.2.2.5)$$

Since anisole (B) was used in large excess over lauric acid (A), there was a chance of external resistance for the transfer of lauric acid from the bulk liquid phase to the external surface of the catalyst particle. Therefore, the speed of agitation was varied under otherwise identical conditions for a particle size of $< 90 \mu\text{m}$. The effect of speed of agitation was studied

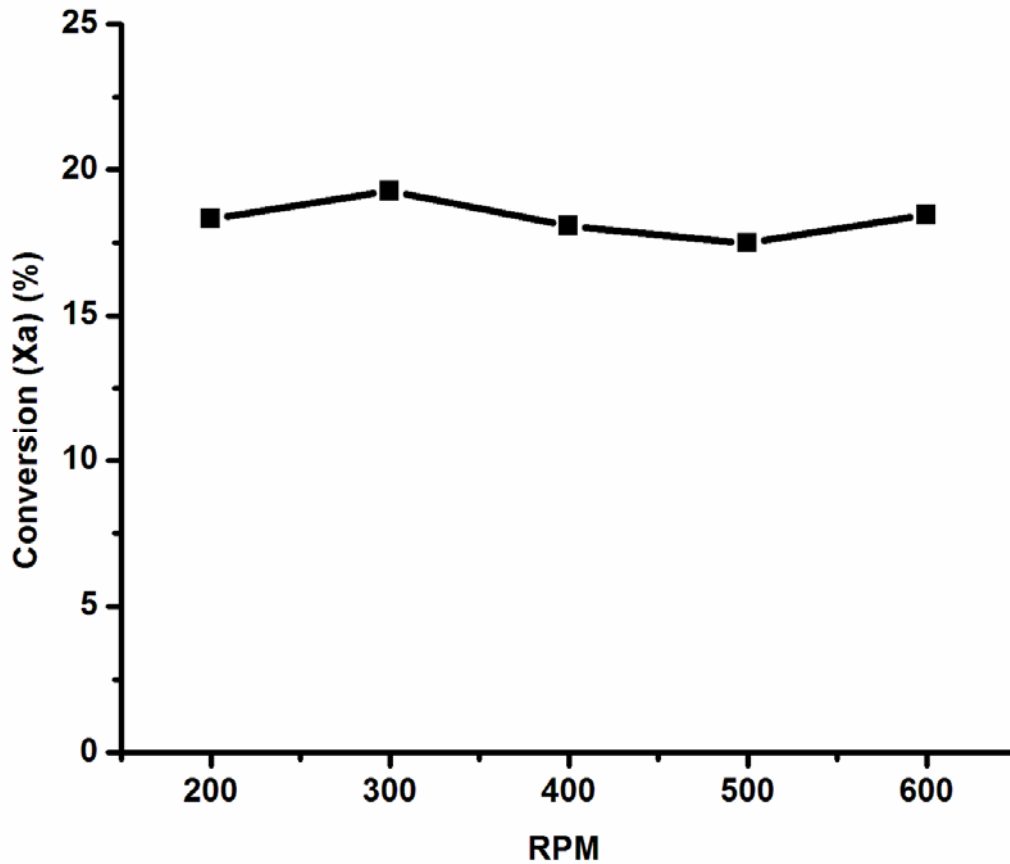


Fig 4.9 Effect of RPM to study external mass transfer in film
 Anisole: C₁₂ acid = 8:1 (mole); Temp = 155 °C; C₁₂: Catalyst = 10:1 (wt.);
 Catalyst = BEA (58)

at a catalyst loading of 16.7 kg/m³ at 155 °C over the range of 200-600 rpm. Fig 4.9 shows the conversion of lauric acid with time. It is seen that the conversion remains practically the same, which indicates the absence of external solid-liquid mass-transfer resistance. Theoretical analysis was also done to ensure that the external mass-transfer resistance was indeed absent as delineated below. The liquid-phase diffusivity values D_{AB} (lauric acid in anisole) and D_{BA} (anisole in lauric acid) were calculated by using the Wilke-Chang equation. The values obtained at 155 °C are as follows:

$$D_{AB} = 7.45 \times 10^{-8} \frac{m^2}{s} \quad (4.2.2.6)$$

$$D_{BA} = 3.61 \times 10^{-8} \frac{m^2}{s} \quad (4.2.2.7)$$

The average particle size used in all experiments was 60 μm . Thus, the particle surface area per unit liquid volume could be calculated from $a_p = 6 \frac{w}{\rho_p d_p}$ as 835 m^{-1} [where w 1.67 kg/m^3 of solid loading, $\rho_p = 2000 \text{ kg}/\text{m}^3$, $d_p = 60\mu\text{m}$].

Thus, the contribution of external mass-transfer coefficient could be calculated. The solid-liquid mass-transfer coefficients for A and B, given as k_a and k_b , respectively, were determined by the Sherwood number correlation. To be on the safe side, the limiting value of the Sherwood number was taken as 2. The actual value is far greater than 2 due to intense agitation. Thus, from the Sherwood number, $Sh = k_s d_p / D$ the solid-liquid mass-transfer coefficients for A and B are calculated as:

$$k_a = 2.48 \times 10^{-3} \text{ m/s} \text{ and } k_b = 1.20 \times 10^{-3} \text{ m/s.}$$

Substituting these values in eqn. no. 4.2.2.5,

$$\frac{1}{k_a a_p [A_0]} = 579.71 \times 10^3 \text{ m}^3 \text{ s/kmol}$$

$$\frac{1}{k_b a_p [B_0]} = 121.41 \times 10^3 \text{ m}^3 \text{ s/kmol}$$

$$\frac{1}{r_{obs}} = 33.76 \times 10^6 \text{ m}^3 \text{ s/kmol}$$

From these values it is clear that the condition given by eqn. No. 4.2.2.5 is satisfied. That is, the rate of solid- liquid mass transfer is much higher than the observed rate of the reaction, and it can be said that the reaction is either surface-reaction controlled or intraparticle-diffusion controlled. Thus, the effect of temperature was studied to find out which of the two was controlling.

4.2.4 Effect of temperature

Fig 4.10 presents the effect of reaction temperature on the acylation reaction over BEA(58). The reaction was carried out at 140, 145 and 155 $^{\circ}\text{C}$. Lauric acid conversion increases steadily with temperature. As the boiling point of anisole is 155 $^{\circ}\text{C}$ and reaction was carried out in a glass reactor (2 necked RB flask), the reaction could not be studied at higher temperatures.

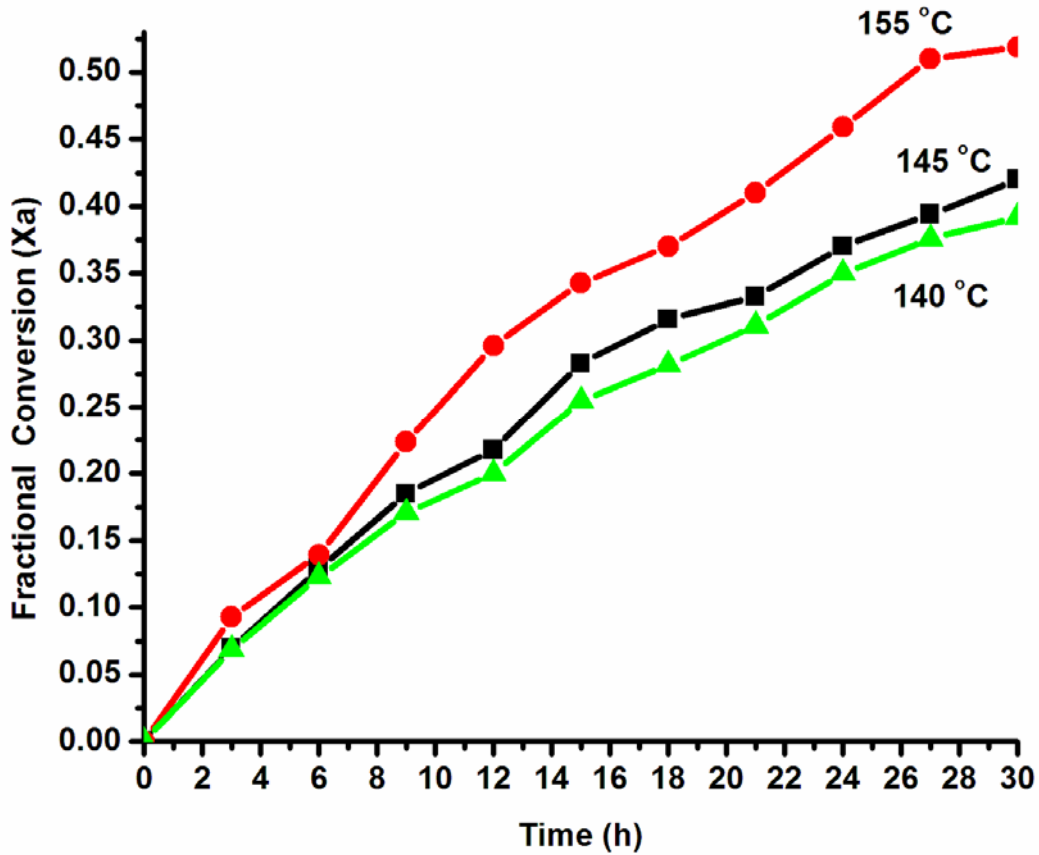


Fig 4.10 Effect of temperature on acylation reaction

Anisole: C₁₂ acid = 8:1 (mole); Temp = 155 °C, 145 °C & 140 °C; C₁₂: Catalyst = 10:1 (wt); Catalyst = BEA (58)

Generally Activation energy is determined from kinetic rate constant 'k', by using the Arrhenius equation. Since the order of reaction was not known, the activation energy was calculated from the general relation (eqn. no. 4.2.3.1) between observed rate and reaction temperature at constant concentration. Rate values used were at 0 h.

$$\text{rate } r_a = f(T, \text{Conc.}) \quad 4.2.3.1$$

i.e,

$$\text{rate } r_a \propto k_0 \exp \frac{-E_a}{RT} * \text{Conc}^n \quad 4.2.3.2$$

Thus the plot between log (rate) versus 1/T by eq. 4.2.3.3 should yield a straight with slope (-E_a/ RT).

$$\ln(r_a) = \ln(k_0 * \text{Conc}^n) - \frac{E_a}{RT}$$

4.2.3.3

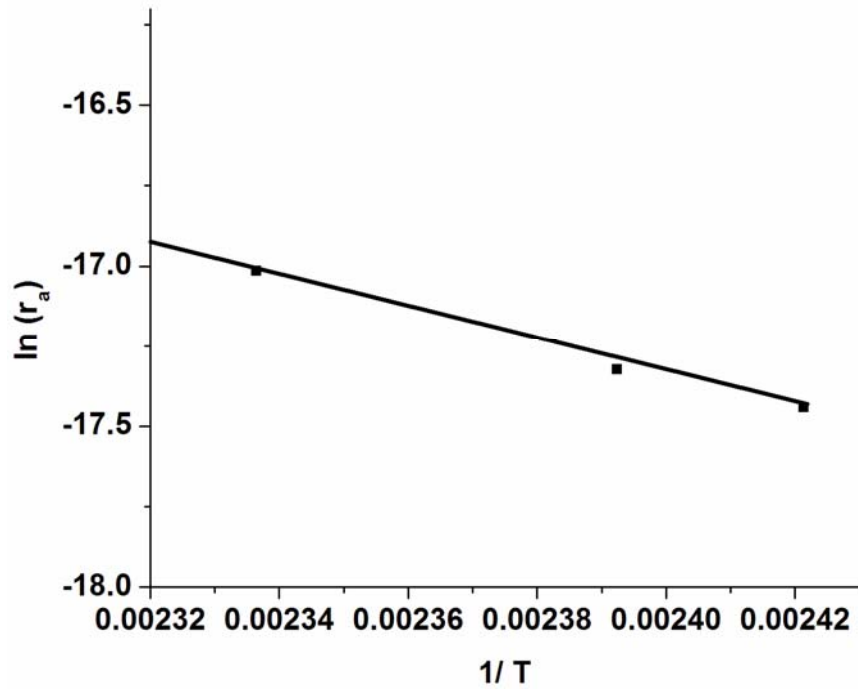


Fig 4.11 Arrhenius plot for acylation reaction

The slope yields

$$\rightarrow -\frac{E_a}{R} = -5087.7$$

$$\rightarrow -E_a = -4135.3 \times 8.314 = -42305 \frac{\text{KJ}}{\text{Kmol K}}$$

$$\rightarrow E_a = 10.2 \frac{\text{Kcal}}{\text{mol K}}$$

The somewhat small value of E_a and the absence of external mass transfer resistance indicates that the reaction might be controlled by pore diffusion effects and fitting the kinetic data into any specific order might not be meaningful. However, it was noticed that the reaction rate did reasonably fit a pseudo I order equation in many cases.

4.2.5 Effect of molar ratio (Anisole: C_{12}) on C_{12} acid conversion

The effect of changing the anisole/lauric acid molar ratio (A/LA) on conversion is plotted in Fig.4.12. A fourfold increase in conversion (at 24 hours) is noticed on increasing the molar ratio two fold from A/LA, 4:1 to 8:1. This means that the overall productivity of the ketone is more in the dilute reaction mixture (8:1) than in the more concentrated (4:1) mixture. Such an effect is possible if the product ketone has an inhibiting effect by strongly adsorbing on the catalyst surface and a large excess of anisole helps to desorb the ketone formed. The acylated product being a large molecular weight polar compound is very likely to be strongly adsorbed on the active sites. Moreover, the adsorbed ketone can further react, giving larger by-products, which can remain adsorbed and further decrease of the catalytic activity. These products may not only block the acid sites but also cause pore-mouth blocking / restrictions with associated loss of catalytic activity. An excess of the solvent (reactant anisole) helps in decreasing the concentration of adsorbed large molecular weight compounds.

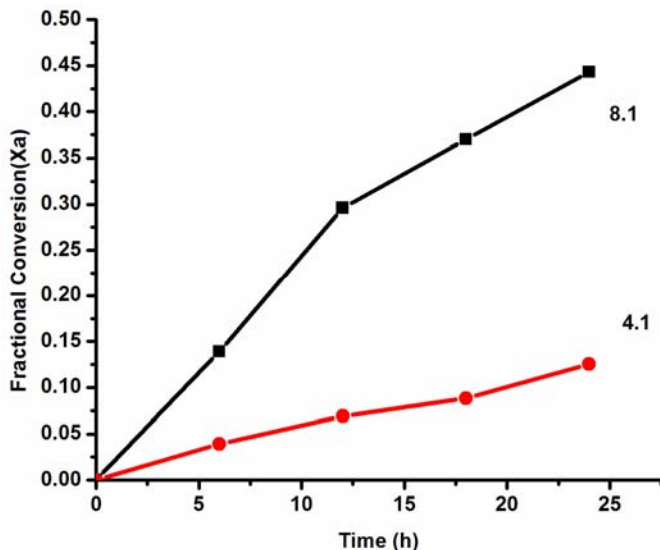


Fig 4.12 Effect of Molar ratio on acylation reaction

Anisole: C₁₂ acid = 8:1 & 4:1 (mole); Temp = 155 °C; C₁₂: Catalyst = 10:1 (wt.);
Catalyst= BEA (SAR 58)

B. HYDROGENATION OF ANISOLE AND ACETOPHENONE

4.3 HYDROGENATION STUDIES

Studies on the hydrogenation of anisole and a model aromatic ketone, acetophenone were carried out to check the possibility of carrying out the hydrogenation of the long chain ketone formed in the acylation reaction to produce a long chain alkyl aromatic compound (lauryl benzene; n-dodecyl benzene) in a single step in the presence of excess anisole. Sulfonic acid derivatives of such long chain n-alkyl benzenes are expected to be useful as highly biodegradable detergents.

The studies were carried out using three supported metal catalysts: 0.5 wt% Pd/BEA(58), 0.5 wt% Ru/BEA(58) and 0.5 wt% Pd/NaY(5.1). Two metals with different hydrogenation characteristics and two supports with different acidic-basic properties have been used. The basic Na-Y(5.1) and acidic BEA(58) supports are expected to have different effects on the hydrogenation activity of the metal function through different metal-support interactions.

4.3.1 Characterization of the catalysts:

The NaY(5.1) used was a commercial sample (CBV100, Zeolyst International) with a total surface area of 735 m²/g and an external surface area of 34 m²/g. The characterization of BEA(58) has already been described. XRD patterns of the metal loaded zeolites were recorded to check if metal loading had any effect on the structural integrity of the zeolites. The XRD patterns (Fig. 4.13 and Fig. 4.14) of the parent zeolites and the metal loaded samples were similar and the metal loading procedure had no effect on the structural integrity of the zeolites.

4.3.2 Hydrogenation reactions

The hydrogenation of anisole and acetophenone was carried out on three metal loaded samples at 25 bars and 155 °C in a Parr (330 ml) autoclave. The results of the studies are described below.

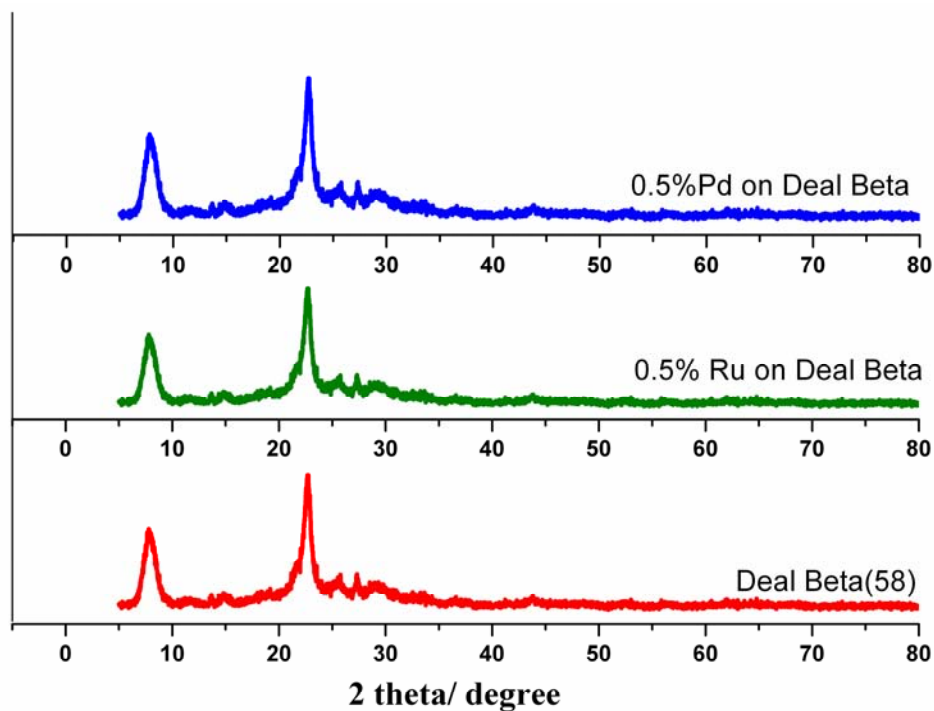


Fig 4.13 X-RAY diffraction patterns for metal loaded BEA(58)

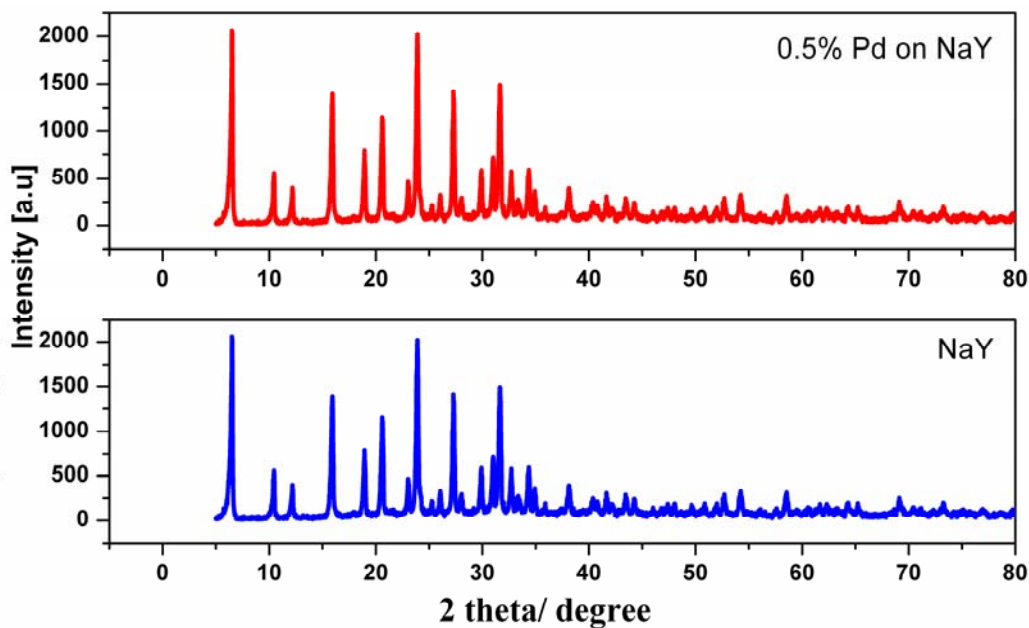


Fig 4.14 X-RAY diffraction patterns for metal loaded NaY(5.1)

4.3.3 Hydrogenation of anisole:

The hydrogenation of anisole is expected to yield methoxy cyclohexanone. The conversion of anisole with duration of run over the three catalysts is presented in Fig 4.15. Product analysis of the reaction mixture (Table 4.6) does not reveal the

formation of the expected methoxy cyclohexanone. The major reaction is the formation of phenol through cleavage of the $-O-Me$ ether linkage, hydrogenation of the phenol to cyclohexanol and its subsequent dimerization as shown in Fig. 4.16. An examination of Fig 4.15 and Table 4.6 reveal that Pd/BEA(58) is more active than Pd/NaY(5.1). Ru/BEA(58) is the least active. However, interestingly, the dimerization reaction (to produce 2-cyclohexyl cyclohexanone) is very small over the NaY(5.1) catalyst, revealing that acid sites are necessary for dimerization of the cyclohexanol formed. The Ru/BEA(58) does not also produce the dimeric ketone because it does hydrogenate the intermediate phenol into cyclohexanol. Similar results have already been reported by earlier workers (Marchenko et.al, 1986)

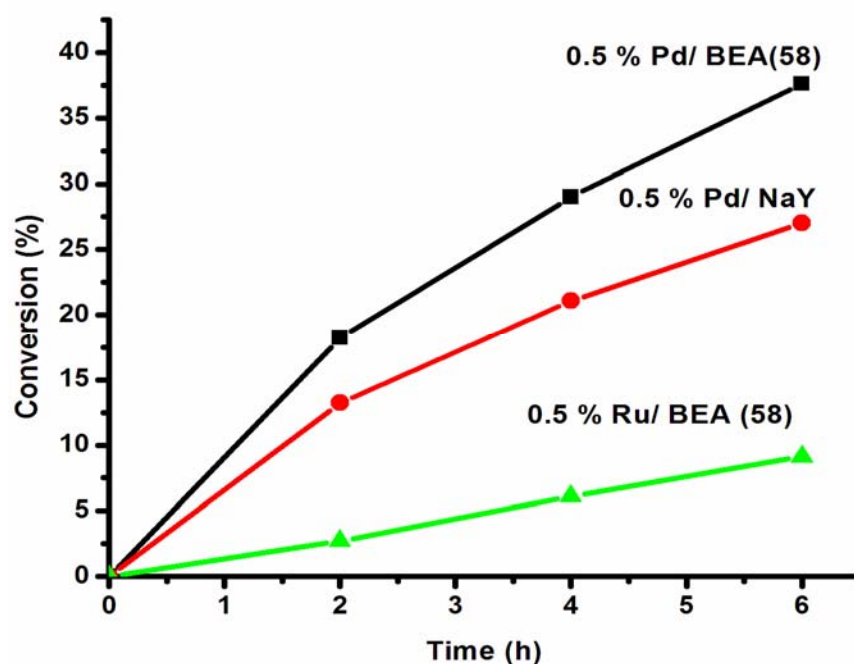


Fig 4.15 Hydrogenation of anisole

Hydrogenation of anisole; Press (H_2) = 25 bar Temp = 155 °C; 500 mg catalyst; 400 RPM

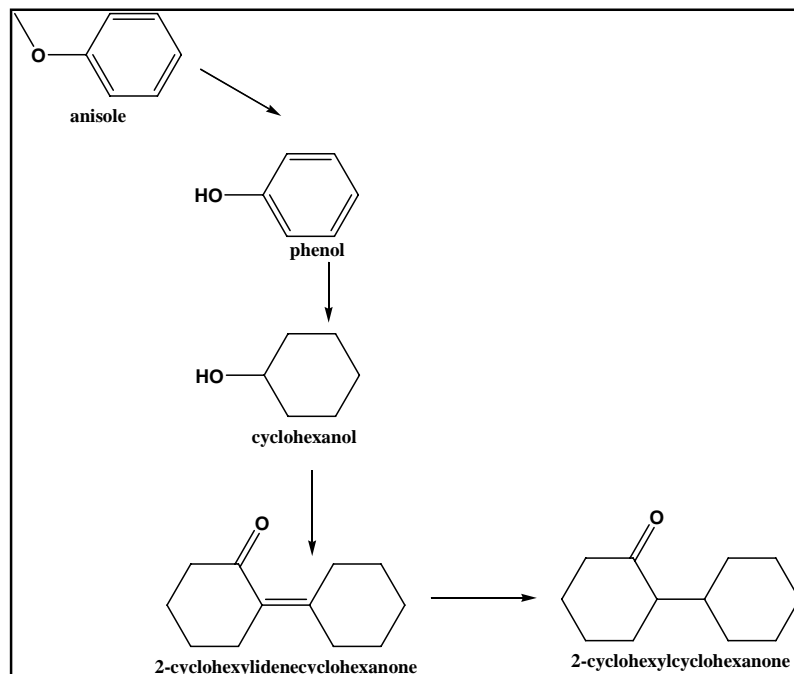


Fig. 4.16 Scheme for formation of the observed products in the hydrogenation of anisole

Table 4.6 Product distribution in hydrogenation of anisole over different catalysts

Samples	Product distribution (area %)				Conversion (mole %)
	Phenol	Cyclohexanol	Dimeric ketone	others	
0.5%Pd/BEA(58)	8.2	17.8	69.4	4.6	37.6
0.5% Pd/ NaY(5.1)()	3.1	77.9	5.7	13.3	27.1
0.5% Ru/BEA(58)	66.3	2.2	--	11.7	9.1

Press = 25 bar H₂; Temp = 155 ° C; 500 mg catalyst; 400 RPM; Time = 6 h.

4.3.4 Hydrogenation of acetophenone

Acetophenone was chosen as the model compound to check its hydrogenation characteristics. The results of these studies are presented in Fig 4.17 and Table 4.7. The studies reveal that the activity of the three catalysts is in the same order as

observed in the hydrogenation of anisole; the activity decreases in the order Pd-BEA(58) > Pd-NaY(5.1) > Ru-BEA(58).

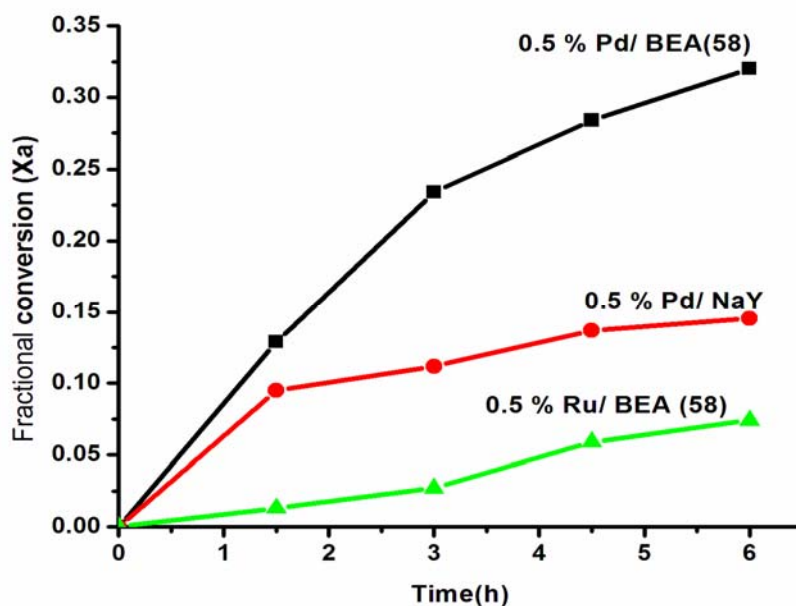


Fig. 4.17 Hydrogenation of acetophenone

Press= 25 bar H₂; Temp = 155 °C; 500 mg catalysts; 400 RPM

The main product of hydrogenation of acetophenone is ethyl benzene in the case of the acidic support, BEA (58) and phenyl ethanol in case of the basic support, NaY(5.1).

Table 4.7 Product distribution of hydrogenation of acetophenone over different catalyst

Samples	Product distribution (area %)				Conversion (mole %)
	Ethyl Benzene	Phenyl Ethanol	Toluene	others	
0.5 %Pd/ BEA(58)	61.4	13.5	7.0	18.1	32.0
0.5% Pd/ NaY(5.1)	53.8	42.3	2	17.9	14.5
0.5%Ru/BEA(58)	70.2	17.9	0.9	11.6	7.4

Press= 25 bar H₂; Temp = 155 °C; 500 mg catalysts; 400 RPM; Time = 6 h

The studies reveal that it is possible to carry out the hydrogenation of the ketone to the alkyl benzene using Pd-BEA catalysts. However, carrying out the

reaction in the presence of anisole does not appear to be possible as anisole undergoes conversion into numerous unwanted products. Hence, the idea of carrying out the acylation and hydrogenation reactions in a single pot does not appear to be feasible in this case, though the ketone can be hydrogenated after removal of the anisole from the reaction mixture.

4.3.5 Comparison of the initial reaction rates over different catalysts

In order to study the relative rates of acylation and hydrogenation reactions (at the conditions of the experiments), the initial rates at 0 h obtained from extrapolation of the data presented in earlier sections is presented in Table 4.8. The results show that the hydrogenation of anisole is much faster than the acylation reaction. The rate of hydrogenation acetophenone is of the same order as that anisole. In the case of the large molecular weight ketone formed with lauric acid and anisole [1-(4-methoxyphenyl)dodecane-1-one], the rate is expected to be lower because of steric hinderance as it is associated with aromatic ring on one side and a long chain paraffin on the other side. Hence when hydrogenation of the ketone is attempted in a single pot reaction, anisole is likely to get hydrogenated faster than the ketone (which is also in low concentration in the reaction mixture). Hence, when a single-pot acylation-cum-hydrogenation is carried out over Pd-BEA, the most likely reaction will be the transformation of anisole into many unwanted products instead of its acylation or the subsequent hydrogenation of the ketone. As predicted, when a single-pot acylation-cum-hydrogenation was carried out over 0.5 % Pd-BEA(58), no acylated product was formed; only the typical products formed during the hydrogenation of anisole were found.

Table 4.8 Comparison of the initial rates for acylation and hydrogenation reactions

Reaction	Conditions	Rates (Kmol/l h)
Acylation over BEA(25)	Temp=155 °C; press= 1 bar; Anisole: Lauric Acid= 8;	2×10^{-5}
Acylation over BEA(55)	Temp=155 °C; press= 1 bar; Anisole: Lauric Acid= 8;	3×10^{-5}
Acylation over BEA(88)	Temp=155 °C; press= 1 bar; Anisole: Lauric Acid= 8;	4.5×10^{-6}
Acylation over BEA(170)	Temp=155 °C; press= 1 bar; Anisole: Lauric Acid= 8;	1.4×10^{-6}
Acylation over BEA(DS1)	Temp=155 °C; press= 1 bar; Anisole: Lauric Acid= 8;	4×10^{-5}
Acylation over BEA(DS2)	Temp=155 °C; press= 1 bar; Anisole: Lauric Acid= 8;	2.5×10^{-5}
Acylation over BEA-Fe	Temp=155 °C; press= 1 bar; Anisole: Lauric Acid= 8;	6.5×10^{-5}
Acylation over BEA-Zn	Temp=155 °C; press= 1 bar; Anisole: Lauric Acid= 8;	7.7×10^{-5}
Acylation over BEA-Ce	Temp=155 °C; press= 1 bar; Anisole: Lauric Acid= 8;	5.3×10^{-5}
Anisole Hydrogenation over 0.5% Pd/ BE(58)	Temp=155 °C; press= 25 H ₂ bar; 400 RPM	1.4×10^{-3}
Anisole Hydrogenation over 0.5% Pd/ NaY(5.1)	Temp=155 °C; press= 25 H ₂ bar; 400 RPM	7.9×10^{-4}

Table 4.8 (Continued)

Anisole Hydrogenation over 0.5% Ru/ BEA(58)	Temp=155 °C; press= 25 H ₂ bar; 400 RPM	1.3 x 10 ⁻⁴
Acetophenone hydrogenation over 0.5% Pd/ BEA(58)	Temp=155 °C; press= 25 H ₂ bar; 400 RPM	8 x 10 ⁻⁴
Acetophenone hydrogenation over 0.5% Pd/ NaY(5.1)()	Temp=155 °C; press= 25 H ₂ bar; 400 RPM	4 x 10 ⁻⁴
Acetophenone hydrogenation over 0.5% Ru/ BEA(58)	Temp=155 °C; press= 25 H ₂ bar; 400 RPM	8 x 10 ⁻⁵

5. SUMMARY AND CONCLUSIONS

The Friedel-Crafts acylation of anisole with a long chain fatty acid, dodecanoic acid (lauric acid), has been carried out over zeolite beta (BEA) and its modified forms. The parent BEA sample obtained from Zeolyst International had a $\text{SiO}_2/\text{Al}_2\text{O}_3$ ratio of 25 (SAR = 25). This was modified by dealumination with HNO_3 to yield samples with lower Al contents (SAR values of 58, 88 and 170). Similarly, the sample was also desilicated by extraction of Si with an aqueous solution of TPAOH. The dealuminated samples suffered crystallinity loss to different extents depending on the severity of the treatment. Also, some amount of unit cell shrinkage was also noticed. However, no crystallinity loss or unit cell shrinkage (decrease in d_{302} value) occurred after the desilication treatments. All the dealuminated and desilicated samples had lower surface areas (S_{BET}) than the parent sample. However, these modified samples possessed larger pore volumes, due mainly to increased mesopore volumes, suggesting the creation of mesoporosity on both dealumination and desilication. As a result, the average pore diameters of the samples increased after both the treatments. More interestingly, mild dealumination (to SAR = 58) and desilication treatments increased the micropore volumes also. The acidity of the parent BEA was found to decrease (as expected) with dealumination. The BEA samples were also loaded with about 2 wt% of Fe^{3+} , Zn^{2+} and Ce^{3+} ions by ion-exchanging. The ion-exchange treatments did not affect the zeolite crystallinity.

All the samples were evaluated in the acylation of anisole with lauric acid at different conditions. The conversion of lauric acid (at 155 °C; anisole : acid (mole), 8 : 1; 30 h run duration) was 38 %. It increased on mild dealumination (SAR 58) to 52% and on desilication to 53.6 and 43.1 %. However, severe dealumination to SAR 88 and 170 decreased the activity drastically (respectively) to 11 and 4 %. The increase in activity is attributed to decreased diffusion constraints due to the increase in the amount and average diameter of the mesopores in the mildly dealuminated and desilicated samples. Though the pore volumes (and pore diameters) were also more in the severely dealuminated samples, the decrease in acidity (number of acid sites) decreased conversion. Ion-exchanging BEA with metal ions increased the activity, the Zn-loaded sample being the most active (72.1% conversion) followed by BEA-Fe (67%) and BEA-Ce (59%). The increase in conversion over the metal containing samples could be due to creation of acid sites through hydrolysis of the metal ion and catalysis by the metal ions themselves. The activation energy value for the reaction

over BEA(58) was 10.2 kCal/mole suggesting the possibility of diffusion effects in the acylation reaction. Separate experiments carried out at various stirrer speeds ruled out the occurrence of bulk diffusion suggesting the possibility of the presence of intra-particle diffusion effects. The major product of the acylation was the p-acylated product (ketone). The yields of the three isomers were in the order, p- > o- > m-isomer. As no major differences in the p-/o- ratios over the different catalysts were observed, shape-selectivity effects leading to greater yields of the p-isomer is not likely. These observations suggest the reaction to be kinetically controlled.

It was then planned to carry out a combined acylation-cum-hydrogenation reaction to prepare n-dodecyl benzene. When an experiment was done using 0.5 wt% Pd/BEA(58) at 25bars H₂ and 155 °C, acylation products were not obtained. This reaction was then investigated by carrying out separate experiments on hydrogenation of anisole and a model aromatic ketone, acetophenone, at the same conditions. To study the effect of the metal and the acido-basic nature of the support, three catalysts were prepared with Pd and Ru as the metals and BEA(58) (acidic support) and NaY (basic support). The studies revealed that on the acidic support, anisole underwent hydrogenolysis to yield the ether, which then underwent hydrogenation into cyclohexanol and dimerization over the acid sites. This dimerization reaction did not occur over the basic support. However, hydrogenation of the ketone into ethylbenzene took place with good selectivity over Pd/BEA(58). These studies point out that it is not possible to carry out the acylation of anisole and hydrogenation of the ketone in a single pot, and that the ketone will need to be separated from the anisole prior to its hydrogenation.

Summing up, the studies reveal that BEA modified by mild dealumination / desilication or ion-exchanging with metal ions, like Zn²⁺ or Fe³⁺ is suitable for the acylation of anisole with long chain acids. Also, acylation over BEA produces mainly the p-acylated product (ketone), which is often the desired product. Pd/BEA is a good catalyst for the hydrogenation of the ketone to the alcohol (another desired product) or the alkyl aromatic hydrocarbon.

REFERENCES

Absil, R.; Hatzikos, G. H. Hydrocarbon Conversion Process Using Zeolite Beta Catalysts. U.S. Patent 1998, 5, 833-840.

Aguilar J.; Corma A.; Melo F.; Sastre E. Alkylation of biphenyl with propylene using acid catalysts. *Catal. Today*. 2000; 55, 225-232.

Anonymous. US Zeolite Market Set to Reach \$1 Billion in 2001, Study Says. *Chemical Market Reporter*. New York, Schnell Publishing Company. 1996.

Anonymous. D458, Zeolite, Industry Trends and Worldwide Markets in 2010. Frost & Sullivan. 2001

Bagnasco G. Improving the Selectivity of NH₃ TPD measurements. *J. Catal.* 1996, 159, 249-252.

Barrer R. *Hydrothermal Chemistry of Zeolites*. London, Academic Press. 1982

Bell A.; Pines A. "NMR Techniques in Catalysis" Heinemann eds., Marcel Dekker, Inc. (1994).

Botella P.; Corma A.; Lopez-Nieto M.; Valencia S.; Jacquoty R. Acylation of Toluene with Acetic Anhydride over Beta Zeolites: Influence of Reaction Conditions and Physicochemical Properties of the Catalyst *J. Catal.* 2000, 195, 161-168

Boyapati M.; Mutyala S.; Mannepalli L.; Kompella V.; Acylation of aromatic ethers with acid anhydrides in the presence of cation-exchanged clays. *Appl. Catal. A: Gen.* 1998, 171, 155-160

Breck D.; *Zeolite Molecular Sieves, Structure, Chemistry and Use*. New York, John Wiley and Sons. 1974

S. Brunauer, P.H. Emmett, E. Teller, J. Am. Chem. Soc. 1938,60, 309.

Casagrande M.; Storaro I.; Lenarda M.; and Ganzerla, R. Highly Selective Friedel-Crafts Acylation of 2-metoxynaphthalene catalysed by H-BETA Zeolite. *Appl.Catal. A.* 2000, 201,263-270.

Charles S. *Heterogeneous catalysis in industrial practise.* 2nd edition. McGraw-Hill Inc.1991

Chiu J.; Pine D.; Bishop S.; Chmelka B. Friedel-Crafts alkylation properties of aluminosilica SBA-15 meso/macroporous monoliths and Jamesoporous powders. *J.Catal.* 2004, 221, 400 -412.

Corma A.; Climent J.; Garcia H.; Primo J. Design of Synthetic Zeolites as Catalysts in Organic Reactions. Acylation of Anisole by Acyl Chlorides or Carboxylic Acids over Acid Zeolites. *Appl. Catal. A.*1989, 49,109-123.

Costa C.; Dzikh P.; Lopes J.; Lemos F.; Ribeiro R. Activity acidity relationship in zeolite ZSM-5. Application of Brønsted-type equations. *J. Mol. Catal. A. Chem.*2000, 154,193-201.

Flanigen, E.M. Zeolite and Molecular Sieve An Historical Perspective, in Bekkum, 1991.

Gregg S.; Sing W.; Adsorption Surface Area and Porosity, Academic Press, London, (1982) Ch. 4.

Higgins J.; La Pierre R.; Schlenker J.; Rohrman A.; Wood J.; Kerr G .;Rohrbaugh W.The Framework Topology of Zeolite Beta. *Zeolites.* 1998, 8, 446 - 452.

Heroshi. Y.; Mitsukura Y.; Kobashi H. Microwave-assisted acylation compounds using carboxylic acids and Zeolite catalysts. *J. Mol. Catal. A: Chem.* 2010, 322, 80-86.

Holderich W.; Röseler J.; Heitmann G.; Liebens A. The use of zeolites in the synthesis of fine and intermediate chemicals. *Catal. Today.* 1997, 37, 353-366.

Jansen J.; Creighton E.; Njo S.; Koningsveid H.; Bekkum H On the Remarkable Behavior of Zeolite Beta in Acid Catalysis. *Catal.Today.* 1997,38, 205 - 212.

Juttu G. *Modified Microporous Aluminosilicates as Novel Solid Acid Catalysis.* University of Delaware. Ph.D Thesis.2001.

Marques P.; Gener I.; Ayrault P.; Bordado C.; Lopes M.; Ramôa Ribeiro F.; Guisnet M Infrared spectroscopic studies of the acid properties of dealuminated BEA zeolites, *Micropor.Mesopor.Mater.*2003,60,251-262.

Matias.P.; S'a Couto I.; Grac a.; Lopes M.; Carvalho P.; Ram Foa Ribeiro.; Guisnet M, *Appl .Catal. A: Gen.* doi:10.1016/j.apcata.2011.03.049

Meier W.; Olson D.; Boerlocher C. *Atlas of Zeolite Structure types.* 4th edition Amsterdam, International Zeolite Association. 1996

.Murphy M. *Structural Modification of Zeolite Beta.* University OF New Brunswick. Master Thesis. 1996.

.Narayanan S.; Murthy K. Montmorillonite as a versatile solid acid catalyst for *tert*-butylation of resorcinol. *Appl. Catal. A. Gen.* 2001,213, 273-278.

Nivarthi G.; Seshan K.; Lercher J. The influence of acidity on zeolite H-BEA catalyzed isobutene/n-butene alkylation. *Micropor.Mesopor. Mater* .1998, 22,379-388.

Roland E.; Kleinschmit P. *Ullman's Encyclopedia of Industrial Chemistry*,VCH Verlagsgesellschaft.1996, Vol A28, 475-504.

Sarsani V.; Lyon C.; Hutchenson K.; Harmer M.; Subramaniam B. Continuous acylation of anisole by acetic anhydride in mesoporous solid acid catalysts: Reaction media effects on catalysts deactivation, *J. Catal.* 245, 2007, 184–190

Szostak R. *Molecular Sieves,Principles of synthesis and Identification*.Van Nostrand Reinhold catalysis series, New York. (1989).

Treacy M.; Higgins J.; Ballmoos R. *Collection of Simulated XRD Powder Patterns for Zeolites*. 3rd edition. Amsterdam,Elsevier. 1996.

Van Bekkum H.; Flanigen M.;Jacobs A.; Jensen C, Introduction to zeolite science and practice, 2nd Ed., Elsevier, Amsterdam, 2001.

Wadlinger R.; Kerr G.; Rosinski E. *Synthesis Zeolite Beta*. (U.S. Patent 3, 1967,308, 069).

Wagholikar G.; Niphadkar S.; Mayadevi S.; Sivasanker S.Acylation of anisole with long-chain carboxylic acids over wide pore zeolites. *Appl. Catal. A: Gen.*2007, 317, 250–257

Yadav G.; Doshi N. Alkylation of aniline with methyl-*tert*-butyl ether (MTBE) and *tert*-butanol over solid acids,product distribution and kinetics. *J. Mol. Catal. A.Chem.*2003, 194, 195-209.

Zaiku X.; Jiaqing B.; Yiqing Y.; Qingling C.; Chengfang Z .Effect of treatment with NaAlO₂ solution on the Surface Acid Properties of Zeolite β. *J. Catal.* 2002, 205, 58-66.